producing T cells are a completely separate lineage from Th1 and Th2 cells (Harrington et al., 2005; Park et al., 2005) and play a critical role in the induction of autoimmune diseases such as MS and rheumatoid arthritis (Ishizu et al., 2005; Langrish et al., 2005; Murphy et al., 2003). In this study, the antigen-specific production of IL-17 was markedly suppressed in the fasudil-treated mice. Thus, fasudil's protective effects on EAE may in part be explained by a down-modulation of IL-17 producing encephalitogenic T cells.

Previous studies by Ford et al. (2003) demonstrated that EAE was significantly attenuated in $CD43^{-/-}$ mice due to decreased lymphocyte trafficking to the CNS and affected T cell differentiation and cytokine production, as myelin-specific $CD43^{-/-}$ $CD4^{+}$ T cells exhibited reduced IFN-γ and increased IL-4 production. CD43 has been implicated in the regulation of both T cell homing and activation (Cullinan et al., 2002; Ostberg et al., 1998) and has been shown to move away from the immunological synapse between T cells and APCs, where ERM function is necessary (Allenspach et al., 2001). In fact, the temporal and spatial alteration of ERM activity, regulated by its dephosphorylation and rephosphorylation, is suggested to be critical for immunological synapse formation and T cell activation through its binding states to many transmembrane proteins, such as CD43 (Cullinan et al., 2002). Inhibition of ERM function thus decreases production of IFN-γ and IL-2 (Allenspach et al., 2001). Thus, suppression of ERM by fasudil *in vivo*, as shown in the present study, may also contribute to the amelioration of EAE partly through a down-regulation of Th1 cytokine.

Increasing evidence suggests that Rho-kinase induces retraction of axons while fasudil facilitates axonal growth through inhibition of the kinase (Mueller et al., 2005; Sakisaka et al., 2004). Previous studies by Wolf et al. (2001) demonstrated that Rho-kinase also regulates oligodendrocyte process formation. Expression of dominant negative Rho in primary oligodendrocytes caused a hyperextension of processes, whereas constitutively activated Rho reduced process formation. As fasudil was shown to transfer intrathecally (Hanada et al., 2005), fasudil may offer the possibility of functional recovery of EAE through facilitation of axonal growth and myelination. Since inflammatory stimuli up-regulated Rho-kinase expression (Hiroki et al., 2004) and Rho was shown to be up-regulated in MS plaques (Tajouri et al., 2003), direct inhibition of Rho-kinase is expected to be beneficial through not only a suppression of inflammatory cell infiltration into the CNS but also neuroregeneration. A marked reduction in the clinical disability and preservation of neurites in the chronic EAE model treated after the first attack with fasudil may suggest that this is plausible. As it is possible that HMG-CoA reductase inhibition by statins induces neurite loss and subsequent neuronal death (Schulz et al., 2004) and cholesterol is indispensable for myelination (Saher et al., 2005), Rho-kinase inhibitors may be more favorable than statins for MS.

Thus, our results indicate a beneficial role of selective blockade of Rho-kinase in autoimmune inflammation of the CNS and may provide a rationale for oral use of fasudil, which has been used with minimal side effects in more than 30,000 patients with subarachnoid hemorrhage (Mueller et al., 2005), in the treatment of MS. Although in an animal model of cardiovascular diseases, high dose fasudil (100 mg/kg/day), like in our study, was applied with the drinking water (Higashi et al., 2003; Abe et al., 2004), low dose fasudil (80 mg three times daily) has been reported to be effective and safe in human cardiovascular diseases (Vicari et al., 2005). Further study of low dose fasudil is called for.

Acknowledgements

This work was supported in part by grants from the Ministry of Education, Culture, Sports, Science and Technology of Japan, a Neuroimmunological Disease Research Committee grant from the Ministry of Health, Labour and Welfare of Japan for Research on Brain Science.

References

Abe, K., Shimokawa, H., Morikawa, K., Uwatoku, T., Oi, K., Matsumoto, Y., Hattori, T., Nakashima, Y., Kaibuchi, K., Sueishi, K., Takeshita, A., 2004. Long-term treatment with a Rho-kinase inhibitor improves monocrotaline-induced fatal pulmonary hypertension in rats. Circ. Res. 94, 385–393.

Adachi, T., Vita, R., Sannohe, S., Stafford, S., Alam, R., Kayaba, H., Chihara, J., 2001. The functional role of Rho and Rho-associated coiled-coil forming protein kinase in eotaxin signaling of eosinophils. J. Immunol. 167, 4609–4615.

Aihara, M., Dobashi, K., Iizuka, K., Nakazawa, T., Mori, M., 2003. Comparison of effects of Y-27632 and Isoproterenol on release of cytokines from human peripheral T cells. Int. Immunopharmacol. 3, 1619–1625.

Aktas, O., Waiczies, S., Smorodchenko, A., Dorr, J., Seeger, B., Prozorovski, T., Sallach, S., Endres, M., Brocke, S., Nitsch, R., Zipp, F., 2003. Treatment of relapsing paralysis in experimental encephalomyelitis by targeting Th1 cells through atorvastatin. J. Exp. Med. 197, 725–733.

Alblas, J., Ulfman, L., Hordijk, P., Koenderman, L., 2001. Activation of Rho and ROCK are essential for detachment of migrating leukocytes. Mol. Biol. Cell 12, 2137–2145.

Allenspach, E.J., Cullinan, P., Tong, J., Tang, Q., Tesciuba, A.G., Cannon, J.L., Takahashi, S.M., Morgan, R., Burkhardt, J.K., Sperling, A.I., 2001. ERM-dependent movement of CD43 defines a novel protein complex distal to the immunological synapse. Immunity 15, 739–750.

Amano, M., Fukata, Y., Kaibuchi, K., 2000. Regulation and functions of Rho-associated kinase. Exp. Cell Res. 261, 44–51.

Bardi, G., Niggli, V., Loetscher, P., 2003. Rho kinase is required for CCR7-mediated polarization and chemotaxis of T lymphocytes. FEBS Lett. 542, 79–83.

Chrissobolis, S., Budzyn, K., Marley, P.D., Sobey, C.G., 2004. Evidence that estrogen suppresses Rho-kinase function in the cerebral circulation in vivo. Stroke 35, 2200–2205.

Cullinan, P., Sperling, A.I., Burkhardt, J.K., 2002. The distal pole complex: a novel membrane domain distal to the immunological synapse. Immunol. Rev. 189, 111–122.

Ford, M.L., Onami, T.M., Sperling, A.I., Ahmed, R., Evavold, B.D., 2003. CD43 modulates severity and onset of experimental autoimmune encephalomyelitis. J. Immunol. 171, 6527–6533.

Fukata, Y., Amano, M., Kaibuchi, K., 2001. Rho–Rho-kinase pathway in smooth muscle contraction and cytoskeletal reorganization of non-muscle cells. Trends Pharmacol. Sci. 22, 32–39.

Greenwood, J., Walters, C.E., Pryce, G., Kanuga, N., Beraud, E., Baker, D., Adamson, P., 2003. Lovastatin inhibits brain endothelial cell Rho-

mediated lymphocyte migration and attenuates experimental autoimmune encephalomyelitis. FASEB J. 17, 905–907.
Hall, A., 1998. Rho GTPases and the actin cytoskeleton. Science 279, 509–514.
Hanada, Y., Kudo, H., Kohmura, E., 2005. Chronologic changes of fasudil hydrochloride and hydroxyfasudil in cerebrospinal fluid of patients with aneurismal subarachnoid hemorrhage. J. Stroke Cerebrovasc. Dis. 14, 47–49.
Harrington, L.E., Hatton, R.D., Mangan, P.R., Turner, H., Murphy, T.L., Murphy, K.M., Weaver, C.T., 2005. Interleukin 17-producing CD4+ effector T cells develop via a lineage distinct from the T helper type 1 and 2 lineages. Nat. Immunol. 6, 1123–1132.
Hendriks, J.J., Alblas, J., van der Pol, S.M., van Tol, E.A., Dijkstra, C.D., de Vries, H.E., 2004. Flavonoids influence monocytic GTPase activity and are protective in experimental allergic encephalitis. J. Exp. Med. 200, 1667–1672.
Higashi, M., Shimokawa, H., Hattori, T., Hiroki, J., Mukai, Y., Morikawa, K., Ichiki, T., Takahashi, S., Takeshita, A., 2003. Long-term inhibition of Rho-kinase suppresses angiotensin II-induced cardiovascular hypertrophy in rats in vivo: effect on endothelial NAD(P)H oxidase system. Circ. Res. 93, 767–775.
Hiroki, J., Shimokawa, H., Higashi, M., Morikawa, K., Kandabashi, T., Kawamura, N., Kubota, T., Ichiki, T., Amano, M., Kaibuchi, K., Takeshita, A., 2004. Inflammatory stimuli upregulate Rho-kinase in human coronary vascular smooth muscle cells. J. Mol. Cell Cardiol. 37, 537–546.
Hiroki, J., Shimokawa, H., Mukai, Y., Ichiki, T., Takeshita, A., 2005. Divergent effects of estrogen and nicotine on Rho-kinase expression in human coronary vascular smooth muscle cells. Biochem. Biophys. Res. Commun. 326, 154–159.
Ishizu, T., Osoegawa, M., Mei, F.J., Kikuchi, H., Tanaka, M., Takakura, Y., Minohara, M., Murai, H., Mihara, F., Taniwaki, T., Kira, J., 2005. Intrathecal activation of the IL-17/IL-8 axis in opticospinal multiple sclerosis. Brain 128, 988–1002.
Kaibuchi, K., Kuroda, S., Amano, M., 1999. Regulation of the cytoskeleton and cell adhesion by the Rho family GTPases in mammalian cells. Ann. Rev. Biochem. 68, 459–486.
Kikuchi, H., Doh-ura, K., Kawashima, T., Kira, J., Iwaki, T., 1999. Immunohistochemical analysis of spinal cord lesions in amyotrophic lateral sclerosis using microtubule-associated protein 2 (MAP2) antibodies. Acta Neuropathol. (Berl) 97, 13–21.
Langrish, C.L., Chen, Y., Blumenschein, W.M., Mattson, J., Basham, B., Sedgwick, J.D., McClanahan, T., Kastelein, R.A., Cua, D.J., 2005. IL-23 drives a pathogenic T cell population that induces autoimmune inflammation. J. Exp. Med. 201, 233–240.
Minohara, M., Ochi, H., Matsushita, S., Irie, A., Nishimura, Y., Kira, J., 2001. Differences between T-cell reactivities to major myelin protein-derived peptides in opticospinal and conventional forms of multiple sclerosis and healthy controls. Tissue Antigens 57, 447–456.
Mueller, B.K., Mack, H., Teusch, N., 2005. Rho kinase, a promising drug target for neurological disorders. Nat. Rev. Drug Discov. 4, 387–398.
Murphy, C.A., Langrish, C.L., Chen, Y., Blumenschein, W., McClanahan, T., Kastelein, R.A., Sedgwick, J.D., Cua, D.J., 2003. Divergent pro- and antiinflammatory roles for IL-23 and IL-12 in joint autoimmune inflammation. J. Exp. Med. 198, 1951–1957.
Nath, N., Giri, S., Prasad, R., Singh, A.K., Singh, I., 2004. Potential targets of 3-hydroxy-3-methylglutaryl coenzyme A reductase inhibitor for multiple sclerosis therapy. J. Immunol. 172, 1273–1286.
Neuhaus, O., Stuve, O., Zamvil, S.S., Hartung, H.P., 2004. Are statins a treatment option for multiple sclerosis? Lancet Neurol. 3, 369–371.
Niggli, V., 1999. Rho-kinase in human neutrophils: a role in signalling for myosin light chain phosphorylation and cell migration. FEBS Lett. 445, 69–72.
Offner, H., 2004. Neuroimmunoprotective effects of estrogen and derivatives in experimental autoimmune encephalomyelitis: therapeutic implications for multiple sclerosis. J. Neurosci. Res. 78, 603–624.
Ostberg, J.R., Barth, R.K., Frelinger, J.G., 1998. The Roman god Janus: a paradigm for the function of CD43. Immunol. Today 19, 546–550.
Park, H., Li, Z., Yang, X.O., Chang, S.H., Nurieva, R., Wang, Y.H., Wang, Y., Hood, L., Zhu, Z., Tian, Q., Dong, C., 2005. A distinct lineage of CD4 T cells regulates tissue inflammation by producing interleukin 17. Nat. Immunol. 6, 1133–1141.
Pluchino, S., Quattrini, A., Brambilla, E., Gritti, A., Salani, G., Dina, G., Galli, R., Del Carro, U., Amadio, S., Bergami, A., Furlan, R., Comi, G., Vescovi, A.L., Martino, G., 2003. Injection of adult neurospheres induces recovery in a chronic model of multiple sclerosis. Nature 422, 688–694.
Saher, G., Brugger, B., Lappe-Siefke, C., Mobius, W., Tozawa, R., Wehr, M.C., Wieland, F., Ishibashi, S., Nave, K.A., 2005. High cholesterol level is essential for myelin membrane growth. Nat. Neurosci. 8, 468–475.
Sakisaka, T., Baba, T., Tanaka, S., Izumi, G., Yasumi, M., Takai, Y., 2004. Regulation of SNAREs by tomosyn and ROCK: implication in extension and retraction of neurites. J. Cell Biol. 166, 17–25.
Schulz, J.G., Bosel, J., Stoeckel, M., Megow, D., Dirnagl, U., Endres, M., 2004. HMG-CoA reductase inhibition causes neurite loss by interfering with geranylgeranylpyrophosphate synthesis. J. Neurochem. 89, 24–32.
Shimokawa, H., Takeshita, A., 2005. Rho-kinase is an important therapeutic target in cardiovascular medicine. Arterioscler. Thromb. Vasc. Biol. 25, 1767–1775.
Stanislaus, R., Pahan, K., Singh, A.K., Singh, I., 1999. Amelioration of experimental allergic encephalomyelitis in Lewis rats by lovastatin. Neurosci. Lett. 269, 71–74.
Tachibana, E., Harada, T., Shibuya, M., Saito, K., Takayasu, M., Suzuki, Y., Yoshida, J., 1999. Intra-arterial infusion of fasudil hydrochloride for treating vasospasm following subarachnoid haemorrhage. Acta Neurochir. (Wien) 141, 13–19.
Tajouri, L., Mellick, A.S., Ashton, K.J., Tannenberg, A.E., Nagra, R.M., Tourtellotte, W.W., Griffiths, L.R., 2003. Quantitative and qualitative changes in gene expression patterns characterize the activity of plaques in multiple sclerosis. Brain Res. Mol. Brain Res. 119, 170–183.
Tharaux, P.L., Bukoski, R.C., Rocha, P.N., Crowley, S.D., Ruiz, P., Nataraj, C., Howell, D.N., Kaibuchi, K., Spurney, R.F., Coffman, T.M., 2003. Rho kinase promotes alloimmune responses by regulating the proliferation and structure of T cells. J. Immunol. 171, 96–105.
Vicari, R.M., Chaitman, B., Keefe, D., Smith, W.B., Chrysant, S.G., Tonkon, M.J., Bittar, N., Weiss, R.J., Morales-Ballejo, H., Thadani, U., 2005. Efficacy and safety of fasudil in patients with stable angina. J. Am. Coll. Cardiol. 46, 1803–1811.
Vollmer, T., Key, L., Durkalski, V., Tyor, W., Corboy, J., Markovic-Plese, S., Preiningerova, J., Rizzo, M., Singh, I., 2004. Oral simvastatin treatment in relapsing-remitting multiple sclerosis. Lancet 363, 1607–1608.
Walters, C.E., Pryce, G., Hankey, D.J., Sebti, S.M., Hamilton, A.D., Baker, D., Greenwood, J., Adamson, P., 2002. Inhibition of Rho GTPases with protein prenyltransferase inhibitors prevents leukocyte recruitment to the central nervous system and attenuates clinical signs of disease in an animal model of multiple sclerosis. J. Immunol. 168, 4087–4094.
Weitz-Schmidt, G., Welzenbach, K., Brinkmann, V., Kamata, T., Kallen, J., Bruns, C., Cottens, S., Takada, Y., Hommel, U., 2001. Statins selectively inhibit leukocyte function antigen-1 by binding to a novel regulatory integrin site. Nat. Med. 7, 687–692.
Wolf, R.M., Wilkes, J.J., Chao, M.V., Resh, M.D., 2001. Tyrosine phosphorylation of p190 RhoGAP by Fyn regulates oligodendrocyte differentiation. J. Neurobiol. 49, 62–78.
Youssef, S., Stuve, O., Patarroyo, J.C., Ruiz, P.J., Radosevich, J.L., Hur, E.M., Bravo, M., Mitchell, D.J., Sobel, R.A., Steinman, L., Zamvil, S.S., 2002. The HMG-CoA reductase inhibitor, atorvastatin, promotes a Th2 bias and reverses paralysis in central nervous system autoimmune disease. Nature 420, 78–84.

ELSEVIER

Journal of Neuroimmunology 184 (2007) 227–231

Journal of
Neuroimmunology

www.elsevier.com/locate/jneuroim

Short communication

Helicobacter pylori infection is a potential protective factor against conventional multiple sclerosis in the Japanese population

Wei Li, Motozumi Minohara, Jen Jen Su, Takeshi Matsuoka, Manabu Osoegawa, Takaaki Ishizu, Jun-ichi Kira *

Department of Neurology, Neurological Institute, Graduate School of Medical Sciences, Kyushu University, Fukuoka 812–8582, Japan

Received 19 September 2006; received in revised form 7 December 2006; accepted 19 December 2006

Abstract

Persistent *Helicobacter pylori* (*H. pylori*) infection is a chronic inflammatory stimulus to hosts with an inverse correlation to atopic disorders. In this study, a total of 105 consecutive multiple sclerosis (MS) patients were divided into 52 opticospinal MS (OSMS) and 53 conventional MS (CMS), and their sera, along with those from 85 healthy controls (HC), were examined by an enzyme-linked immunosorbent assay using antibodies against *H. pylori*. *H. pylori* seropositivity was significantly lower in patients with CMS (22.6%) compared with HC (42.4%) and patients with OSMS (51.9%) ($p=0.0180$ and $p=0.0019$, respectively). In patients with CMS, *H. pylori* seropositivity showed a significant inverse association with mean EDSS score and fulfillment of McDonald MRI criteria for space (OR=0.61, $p=0.0344$ and OR=0.11, $p=0.0297$). These findings suggest that *H. pylori* infection is a protective factor against CMS in Japanese.

Keywords: Multiple sclerosis; *Helicobacter pylori*; Japanese; Opticospinal MS

1. Introduction

Multiple sclerosis (MS) is the most common inflammatory demyelinating disease of the central nervous system (CNS) in humans. MS in Asians is characterized by a low prevalence rate and selective involvement of the optic nerve and spinal cord. Opticospinal MS (OSMS) is observed in 15–40% of Japanese MS patients, with the remainder having features that are similar to those of MS in Caucasians (conventional or classical MS; CMS) (Kira, 2003). Recently, a sharp rise in the ratio of CMS to OSMS in the Japanese population was reported, especially among those born after Japan's period of rapid economic growth, together with an increase in the overall prevalence of MS (Kira et al., 1999; Kira, 2003). Although the etiology of MS is unknown, the environment during childhood has a critical effect on the susceptibility to MS (Compston, 1997). Therefore, environmental changes accompanied with Japan's Westernization may have altered the incidence and phenotypes of MS in Japanese.

Helicobacter pylori (*H. pylori*) are gram-negative microaerophilic bacteria that reside in the stomachs of more than 50% of the entire human population (Blaser, 1993). *H. pylori* infection has been reported to have an inverse correlation with the prevalence of atopic disorders (McCune et al., 2003), which is consistent with the hygiene hypothesis; that is, that an early childhood infection can suppress allergic disorders (Cremonini and Gasbarrini, 2003). The present study was designed to reveal the prevalence of *H. pylori* infection in each MS subtype in the Japanese population.

2. Subjects and methods

2.1. Subjects

A total of 105 consecutive patients (24 men and 81 women) with MS, diagnosed at the Department of Neurology,

* Corresponding author. Tel.: +81 92 642 5340; fax: +81 92 642 5352.
E-mail address: kira@neuro.med.kyushu-u.ac.jp (J. Kira).

0165-5728/$ - see front matter © 2007 Elsevier B.V. All rights reserved.
doi:10.1016/j.jneuroim.2006.12.010

Kyushu University Hospital according to the criteria of McDonald et al. (2001), were enrolled in this study. The age at examination was 46.9±13.2 years (mean±SD; range: 14 to 73 years) and the age at disease onset was 32.9±14.2 years (range: 9 to 70 years). There were no obvious gastropathy symptoms, such as gastric and duodenal ulcer, at the time of blood sampling. Patients were classified clinically into two subtypes: OSMS or CMS, as described previously (Kira et al., 1996). OSMS diagnosed according to the criteria for OSMS (Kira, 2003). Briefly, 52 patients whose clinically estimated main lesions were confined to both optic nerve and spinal cord were classified as OSMS. These patients had no clinical evidence of disease in either the cerebrum or cerebellum; however, minor brainstem signs, such as transient double vision and nystagmus, were acceptable. The remaining 53 patients had multiple involvement of the CNS, including the cerebrum, cerebellum and brainstem, and were classified as CMS. In addition, eighty-five healthy subjects (21 men and 64 women) were enrolled as healthy control (HC) subjects. Their average age at sampling was 43.5±12.6 years (range: 21 to 64 years). The disability status of patients was scored by one of the authors (TM) using Kurtzke's Expanded Disability Status Scale (EDSS) score (Kurtzke, 1983).

2.2. Anti-H. Pylori antibody assay

The presence in the serum of antibody against *H. pylori* was determined by an ELISA using SMITEST ELISA helicobacter (Chemicon, Australia) according to the manufacturer's instructions. A measure of 50 U/ml was set as the cut-off value for this assay, such that any reading greater than this was considered as a positive *H. pylori* infection.

2.3. Magnetic resonance imaging

All MR studies were performed using a 1.5 T Magnetom Vision and Symphony (Siemens Medical Systems, Erlangen, Germany) MRI system (Su et al., 2006). Brain and spinal cord MRI were evaluated independently by two of the authors (JJS and TM) who were naive to the diagnoses. Brain MRI lesions were evaluated according to McDonald's MRI criteria for MS (McDonald et al., 2001). Spinal cord lesions longer than three vertebral segment lengths were considered to be longitudinally extensive spinal cord lesions (LESCL).

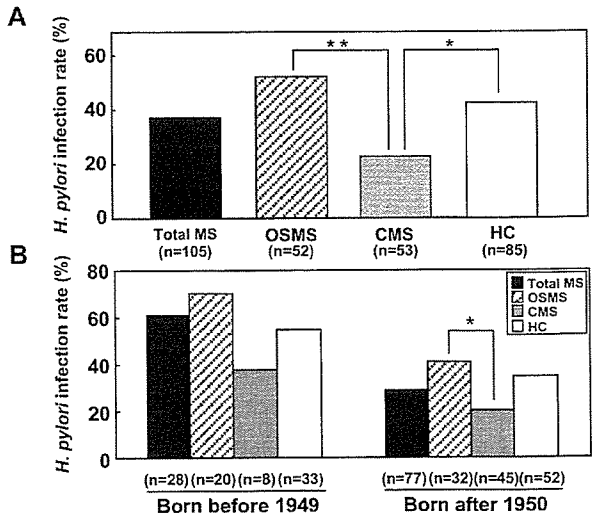

Fig. 1. Frequency of *H. pylori* seropositivity in MS patients and healthy controls. (A) *H. pylori* seropositivity was significantly lower in CMS patients, as compared with OSMS patients and healthy controls (*, $p<0.05$; **, $p<0.005$). (B) *H. pylori* seropositivity was significantly lower in CMS patients than in OSMS patients among those born after 1950 (*, $p<0.05$).

2.4. Statistical analysis

Statistical analyses of ages at onset, blood sampling and final follow-up, disease duration and EDSS scores were initially performed using the Kruskal–Wallis *H* test. When statistical significance was found, the Mann–Whitney *U* test was used to determine the statistical differences between each subgroup. Uncorrelated *p*-values were corrected by multiplying by the number of comparisons (Bonferroni–

Table 1
Demographic features of the subjects

	Total MS (N=105)	OSMS (N=52)	CMS (N=53)	HC (N=85)
Male : Female	24 : 81 (1 : 3.38)	9 : 43 (1 : 4.78)	15 : 23 (1 : 2.53)	21 : 64 (1 : 3.05)
Age at onset (years)[a]	32.9±14.2	36.5±15.0 *	29.4±12.5	NA
Age at blood sampling (years)[a]	41.2±13.2	44.9±13.9 *	37.6±11.5 *	43.5±12.6
Age at final follow-up (years)[a]	46.9±13.2	50.1±14.2 *	43.7±11.4	NA
Disease duration at blood sampling (months)[a]	96.8±89.7	97.3±89.2	96.2±91.0	NA
Disease duration at final follow-up (months)[a]	144.3±102.9	148.5±100.3	140.1±106.1	NA
EDSS scores at final follow-up[a]	4.3±2.6	4.4±2.6	4.2±2.6	NA
Fulfilling McDonald MRI criteria (%)	37.2	19.6 *	57.5	NA
LESCL (%)	35.5	47.9 *	22.2	NA

EDSS: Kurtzke's Expanded Disability Status Scale; LESCL: longitudinally extensive spinal cord lesion; NA: not applicable.
Mean±SD, * $p < 0.05$.

Table 2
Results of logistic regression analysis to predict *H. pylori*-seropositive versus seronegative in MS patients

Variables	Seropositive (N=39)	Seronegative (N=66)	Odds ratio	95% CI	p value
Gender, % female	76.9	77.3	0.59	0.20–1.73	0.3346
Mean age at onset, y (SD)	36.7 (14.8)	30.7 (13.5)	1.28	0.94–1.74	0.1206
Mean age at blood sampling, y (SD)	45.1 (13.6)	38.9 (12.5)	0.81	0.60–1.10	0.1729
Mean duration at blood sampling, y (SD)	8.4 (8.6)	7.9 (6.8)	1.02	0.99–1.04	0.1202
Subtype, % CMS	30.8	62.1	0.29	0.12–0.71	0.0067

CI: confidence interval.

Dunn's correction). The differences between two proportions were tested for significance by Fisher's exact test. Logistic regression analysis was performed to assess the association of MS with the *H. pylori* antibody-positive group and, within each MS subtype, the association of the *H. pylori* positivity with clinical and MRI parameters. In all assays, significance was defined as $p<0.05$.

3. Results

3.1. Demographic features of each subtype of MS

The demographic features of the patients are summarized in Table 1. The ages at onset, at blood sampling and at final follow-up were significantly higher in OSMS patients than in CMS patients ($p=0.0282$, $p=0.0246$, $p=0.0345$, respectively). The disease durations at the time of blood sampling and at final follow-up, and the EDSS at final follow-up, did not differ significantly between OSMS and CMS subtypes. The frequency of patients who fulfilled the McDonald MRI criteria for space was significantly higher in the CMS group than in the OSMS group (57.5% vs. 19.6%, $p=0.0003$), whereas the frequency of LESCL was higher in the OSMS group than in the CMS group (47.9% vs. 22.2%, $p=0.0097$).

3.2. Frequency of H. Pylori seropositivity in MS patients and healthy controls

The frequency of *H. pylori* seropositivity did not differ significantly between MS patients collectively (39/105, 37.1%) and HC (36/85, 42.4%) (Fig. 1). When analyzed separately by clinical phenotype, *H. pylori* seropositivity was significantly lower in CMS patients (12/53, 22.6%), as compared with OSMS patients (27/52, 51.9%) and HC ($p=0.0019$ and $p=0.0180$, respectively). Furthermore, when analyzed separately by year of birth, in patients born after 1950, *H. pylori* seropositive rate was significantly lower in CMS patients (9/45, 20%) than OSMS patients (13/32, 40.6%; $p=0.0483$). On the other hand, in patients born before 1950, although the rate of seropositivity in CMS patients was again about half that of OSMS patients (37.5% vs. 70%), the rates of seropositivity did not differ significantly between the groups, presumably because of the small sample size. Regardless of a birth-date before or after 1950, *H. pylori* seropositivity was lower in patients with CMS compared with HC; however, the difference did not reach statistical significance.

3.3. Relationship between H. Pylori seropositivity and MS subtype

The MS patients were divided into *H. pylori* seropositive and seronegative groups and the demographic parameters, shown in the methods and Table 2, were compared between the two groups by logistic regression analysis. Among the variables examined, *H. pylori* seropositivity showed a significant inverse association with CMS (OR=0.29 [95% CI=0.12 to 0.71], $p=0.0067$) (Table 2). Even when birth before or after 1950 was used as a variable instead of age at blood sampling, *H. pylori* infection had a significant inverse association with CMS (OR=0.321 [95%CI=0.13–0.78], $p=0.0124$).

Table 3

Variables	Seropositive (N=12)	Seronetgative (N=41)	Odds ratio	95% CI	p value
Results of logistic regression analysis to predict H. pylori-seropositive versus seronegative in CMS patients					
Mean duration at final follow-up, y (SD)	12.2 (10.1)	11.5 (8.6)	1.01	0.99–1.02	0.5623
Mean EDSS score, (SD)	3.08 (2.30)	4.59 (2.65)	0.61	0.39–0.96	0.0344
LESCL, %	18.2	23.5	10.50	0.68–163.27	0.0930
Fulfilling McDonald MRI criteria, %	27.3	69.0	0.11	0.02–0.81	0.0297
Variables	Seropositive (N=27)	Seronetgative (N=25)	Odds ratio	95% CI	p value
Results of logistic regression analysis to predict H. pylori-seropositive versus seronegative in OSMS patients					
Mean duration at final follow-up, y (SD)	13.0 (9.4)	11.7 (7.3)	1.00	0.99–1.01	0.4305
Mean EDSS score, (SD)	4.59 (2.57)	4.12 (2.66)	0.93	0.71–1.21	0.5702
LESCL, %	60.0	34.8	3.37	0.81–13.94	0.0939
Fulfilling McDonald MRI criteria, %	18.2	20.8	0.67	0.14–3.26	0.6155

EDSS: Kurtzke's Expanded Disability Status Scale; LESCL: longitudinally extensive spinal cord lesions; CI: confidence interval.

3.4. Relationship between H. Pylori seropositivity and clinical and MRI parameters in each MS subtype

Within the CMS group, among the clinical and MRI parameters examined by logistic regression analysis, *H. pylori* seropositivity demonstrated a significant inverse association with mean EDSS score (OR=0.61 [95% CI=0.39 to 0.96], $p=0.0344$) and fulfillment of McDonald MRI criteria for space (OR=0.11 [95%CI=0.02 to 0.81], $p=0.0297$) (Table 3). On the other hand, no variables were associated with *H. pylori* seropositivity in the OSMS group.

4. Discussion

The present study demonstrates that *H. pylori* infection is significantly lower in patients with CMS than in HC or patients with OSMS. The observation that *H. pylori* infection has a significant inverse association with CMS by logistic regression analysis further supports the notion that *H. pylori* is a protective factor against CMS in Japanese.

In Japanese, the prevalence of *H. pylori* infection is lower in the population born after 1950 than it is in those born before 1950 (Asaka et al., 1992). In our study, *H. pylori* seropositivity was also shown to be lower in subjects born after 1950 than in those born before 1950, in all subject groups. However, differences in *H. pylori* positivity among the three groups demonstrated a similar trend irrespective of date of birth. Furthermore, logistic regression analysis, using birth before or after 1950 as a variable, indicated that *H. pylori* positivity had an inverse association with CMS. There is only one report, in the Polish literature, indicating a lower frequency of *H. pylori* infection in MS as compared with controls (Wender, 2003). As CMS in Asians is considered to be the same as MS in Caucasians, our results are in accord with those of the Polish MS study. On the other hand, OSMS is characterized by a higher age at onset, marked female preponderance, frequent relapses, severe disability, fewer brain MRI lesions, LESCL, marked pleocytosis in the cerebrospinal fluid (CSF) and an absence of oligoclonal bands in the CSF; therefore, it is considered to have a distinct immune mechanism (Kira, 2003).

H. pylori infection is supposed to occur mainly before 2 years of age, primarily because the parietal cells that secrete gastric acids, which hamper the survival of *H. pylori*, are not well matured during infancy (Graham, 1991). Once acquired, the bacterium persists for years and decades (Graham, 1991). Thus, the difference in the frequency of *H. pylori* seropositivity suggests a distinction in the infectious environment during childhood. Therefore, the sanitary environment during childhood is thought to have been different between patients with CMS and those with OSMS; that is, a clean environment is associated with CMS and an infectious one is associated with OSMS.

Individuals infected with *H. pylori* were reported to be 30% less likely to have concomitant allergic diseases (McCune et al., 2003). A protective effect against allergy by *H. pylori* infection is considered to be the result of generic exposure to pathogens, rather than being due to the specific infection. A bacterial infection can influence the balance between T helper 1 (Th1) and T helper 2 (Th2) cells, augmenting a Th1 response while dampening the Th2 response. Thus, infection reduces the frequency of allergic disorders. However, the Th1/Th2 paradigm appears to be an oversimplification. Recent studies have reported that Th1 type autoimmune diseases, such as RA (Kero et al., 2001), Crohn's disease (Kero et al., 2001) and type 1 diabetes mellitus (Stene and Nafstad, 2001), are rather higher in patients that have airway allergies, a Th2 disease, and that both allergic disorders and autoimmune diseases are increasing in parallel. Such an increase occurs in younger generations in developed countries where good sanitation reduces the frequency of childhood infection. Therefore, Th1 and Th2 diseases coexist more frequently in atopic individuals raised in a clean environment. Less frequent bacterial infection is supposed to curtail the development of the immunoregulatory system in children, thereby perpetuating either allergic or autoimmune inflammation (Yazdanbakhsh et al., 2002). Recently, it has been shown that people with more siblings of a younger age have a reduced risk of MS (Ponsonby et al., 2005) suggesting that infection encountered early in life renders individuals resistant to MS. The results of our study appear to be consistent with this. Considering all of these observations together, a lower frequency *of H. pylori* infection might be a reflection of good sanitation, but it would seem to render individuals more susceptible to CMS. In CMS patients, the mean EDSS scores and brain MRI lesions fulfilling McDonald MRI criteria were inversely associated with *H. pylori* positivity, suggesting that *H. pylori* infection is a protective factor against the development of brain lesions and subsequent disability.

In summary, our study indicates a difference in *H. pylori* seropositivity between Japanese patients with OSMS and those with CMS. Although further study is required, these observations suggest that differences in childhood environment might exert distinct effects on the development of each MS subtype later in life.

Acknowledgements

This work was supported by grants from the Ministry of Education, Culture, Sports, Science and Technology, Japan. The Neuroimmunological Disease Research Committee and the Ministry of Health, Labor and Welfare, Japan, for Research on Brain Science.

References

Asaka, M., Kimura, T., Kudo, M., Takeda, H., Mitani, S., Miyazaki, T., Miki, T., Graham, D.Y., 1992. Relationship of *Helicobacter pylori* to serum pepsinogens in an asymptomatic Japanese population. Gastroenterology 102, 760–766.

Blaser, M.J., 1993. *Helicobacter pylori*: microbiology of a 'slow' bacterial infection. Trends Microbiol. 1, 255–259.

Compston, A., 1997. Genetic epidemiology of multiple sclerosis. J. Neurol. Neurosurg. Psychiatry 62, 553–561.

Cremonini, F., Gasbarrini, A., 2003. Atopy, *Helicobacter pylori* and the hygiene hypothesis. Eur. J. Gastroenterol. Hepatol. 15, 635–636.

Graham, D.Y., 1991. *Helicobacter pylori*: its epidemiology and its role in duodenal ulcer disease. J. Gastroenterol. Hepatol. 6, 105–113.

Kero, J., Gissler, M., Hemminki, E., Isolauri, E., 2001. Could TH1 and TH2 diseases coexist? Evaluation of asthma incidence in children with celiac disease, type 1 diabetes, or rheumatoid arthritis: a register study. J. Allergy Clin. Immunol. 108, 781–783.

Kira, J., Kanai, T., Nishimura, Y., Yamasaki, K., Matsushita, S., Kawano, Y., Hasuo, K., Tobimatsu, S., Kobayashi, T., 1996. Western versus Asian types of multiple sclerosis: immunogenetically and clinically distinct disorders. Ann. Neurol. 40, 569–574.

Kira, J., Yamasaki, K., Horiuchi, I., Ohyagi, Y., Taniwaki, T., Kawano, Y., 1999. Changes in the clinical phenotypes of multiple sclerosis during the past 50 years in Japan. J. Neurol. Sci. 166, 53–57.

Kira, J., 2003. Multiple sclerosis in the Japanese population. Lancet Neurol. 2, 117–127.

Kurtzke, J.F., 1983. Rating neurological impairment in multiple sclerosis: an expanded disability status scale (EDSS). Neurology 33, 1444–1452.

McCune, A., Lane, A., Murray, L., Harvey, I., Nair, P., Donovan, J., Harvey, R., 2003. Reduced risk of atopic disorders in adults with *Helicobacter pylori* infection. Eur. J. Gastroenterol. Hepatol. 15, 637–640.

McDonald, W.I., Compston, A., Edan, G., Goodkin, D., Hartung, H.P., Lublin, F.D., McFarland, H.F., Paty, D.W., Polman, C.H., Reingold, S.C., Sandberg-Wollheim, M., Sibley, W., Thompson, A., van den Noort, S., Weinshenker, B.Y., Wolinsky, J.S., 2001. Recommended diagnostic criteria for multiple sclerosis: guidelines from the International Panel on the diagnosis of multiple sclerosis. Ann. Neurol. 50, 121–127.

Ponsonby, A.L., van der Mei, I., Dwyer, T., Blizzard, L., Taylor, B., Kemp, A., Simmons, R., Kilpatrick, T., 2005. Exposure to infant siblings during early life and risk of multiple sclerosis. JAMA 26, 463–469.

Stene, L.C., Nafstad, P., 2001. Relation between occurrence of type 1 diabetes and asthma. Lancet 357, 607–608.

Su, J.J., Osoegawa, M., Matsuoka, T., Minohara, M., Tanaka, M., Ishizu, T., Mihara, F., Taniwaki, T., Kira, J., 2006. Upregulation of vascular growth factors in multiple sclerosis: Correlation with MRI findings. J. Neurol. Sci. 243, 21–30.

Wender, M., 2003. Prevalence of *Helicobacter pylori* infection among patients with multiple sclerosis. Neurol. Neurochir. Pol. 37, 45–48.

Yazdanbakhsh, M., Kremsner, P.G., van Ree, R., 2002. Allergy, parasites, and the hygiene hypothesis. Science 296, 490–494.

ELSEVIER
Journal of the Neurological Sciences xx (2007) xxx–xxx
Journal of the Neurological Sciences
www.elsevier.com/locate/jns

A distinct subgroup of chronic inflammatory demyelinating polyneuropathy with CNS demyelination and a favorable response to immunotherapy

Arnold Angelo M. Pineda [a], Katsuya Ogata [b], Manabu Osoegawa [a], Hiroyuki Murai [a], Hiroshi Shigeto [a], Takashi Yoshiura [c], Shozo Tobimatsu [b], Jun-ichi Kira [a,*]

[a] *Department of Neurology, Neurological Institute, Graduate School of Medical Sciences, Kyushu University, Fukuoka 812-8582, Japan*
[b] *Department of Clinical Neurophysiology, Neurological Institute, Graduate School of Medical Sciences, Kyushu University, Fukuoka 812-8582, Japan*
[c] *Department of Radiology, Kyushu University, Fukuoka 812-8582, Japan*

Received 7 September 2006; received in revised form 18 December 2006; accepted 3 January 2007

Abstract

To explore subclinical central nervous system (CNS) involvement in chronic inflammatory demyelinating polyneuropathy (CIDP), we recorded somatosensory evoked potentials (SEPs) and motor evoked potentials (MEPs) using transcranial magnetic stimulation, to measure central sensory conduction time (CSCT) and central motor conduction time (CMCT) and examined brain and spinal cord MRI in patients with probable CIDP based on the American Academy of Neurology AIDS Task Force criteria. Eighteen patients with probable CIDP (12 males and 6 females; mean age at examination±SD, 45.8±17.0 years; range, 17–72) were included in the study. Of the 13 patients who underwent SEPs, one had prolonged CSCT (8%) and of the 13 who underwent MEPs, four had abnormal CMCT (31%). Cranial MRI revealed five of 18 patients had abnormal scans, only one of which showed multiple ovoid periventricular lesions suggestive of demyelination while none showed any intramedullary lesion on spinal cord MRI. Thus, 6 of the 18 patients were considered to have subclinical demyelinative CNS involvement which had lower disability on Global Neurological Disability Score (GNDS) ($p=0.0061$), a male preponderance (0.0537) and a larger compound muscle action potential (CMAP) amplitude in the median nerve ($p=0.005$) than those without. The decrease of GNDS with immunologic therapies was nearly significant in the former ($p=0.0556$) but not in the latter. The results of the present study suggest that subclinical CNS involvement in CIDP is not uncommon in Japanese patients and that CIDP with subclinical CNS involvement is more demyelinative thus responsive to immunotherapies while those without have more axonal damage and less responsive to immunotherapies.

Keywords: Chronic inflammatory demyelinating polyneuropathy; Motor evoked potentials; Somatosensory evoked potentials; Central nervous system

1. Introduction

Chronic inflammatory demyelinating polyneuropathy (CIDP) is considered to be an autoimmune disorder of the peripheral nervous system (PNS). Although peripheral myelin is targeted by an autoimmune attack, central nervous system (CNS) involvement has been suggested in a fraction of CIDP patients with the presence of subclinical electrophysiologic and magnetic resonance imaging (MRI) abnormalities.

In two large series, CNS involvement was clinically observed in 5% and 8% of patients, respectively [1,2]. In the electrophysiological study by Ormerod et al. [3], six of 18 patients (33%) had unilateral or bilateral abnormalities in central motor conduction time (CMCT) on motor evoked potentials (MEPs). On brain MRI, a third to a half of CIDP patients have been reported to have brain lesions [3–6] whereas demyelinating lesions with typical appearance of multiple sclerosis (MS) are uncommon; for example, two of

* Corresponding author. Tel.: +81 92 642 5340; fax +81 92 642 5352.
E-mail address: kira@neuro.med.kyushu-u.ac.jp (J. Kira).

0022-510X/$ - see front matter © 2007 Elsevier B.V. All rights reserved.
doi:10.1016/j.jns.2007.01.004

Please cite this article as: Pineda AAM et al. A distinct subgroup of chronic inflammatory demyelinating polyneuropathy with CNS demyelination and a favorable response to immunotherapy. J Neurol Sci (2007), doi:10.1016/j.jns.2007.01.004

26 patients (8%) in the series of Hawke et al. [6]. As non-specific brain lesions are frequently encountered on MRI, the electrophysiological methods may be more suitable for detecting demyelinative CNS lesions in CIDP. Therefore, the present study was undertaken firstly to explore subclinical CNS involvement in CIDP patients without clinically overt CNS signs, by electrophysiological methods such as MEPs and somatosensory evoked potentials (SEPs), and by brain and spinal cord MRI. Moreover, it was recently shown that in CIDP patients, treatment response to intravenous immunoglobulin (IVIg) administration was in part determined by degree of peripheral axonal involvement with poor response in those with greater axonal damage [7]. However, it is unknown whether CIDP patients with subclinical CNS involvement respond to immunotherapies well or not. Thus, secondly, we aimed to clarify the difference between patients with subclinical CNS involvement and those without.

2. Subjects and methods

2.1. Subjects

Eighteen consecutive patients with probable CIDP (12 males and six females; mean age at examination±SD, 45.8± 7.0 years; range, 17–72) based on the criteria of the American Academy of Neurology AIDS Task Force were included [8]. The demographic features of the patients are described in Table 1. The mean age of onset was 40.5± 20.7 years (mean±SD; range 17–72 years). The duration of disease ranged from 2 months to 36 years (mean±SD= 5.8±10.9 years). Seven presented with weakness while eleven with combined weakness and sensory impairment. At some stage in the clinical course, all of the patients showed distal limb weakness while sensory disturbance was present in 15. None of the patients had clinical signs of CNS involvement. The clinical courses were chronic progressive in 10 patients, relapsing–remitting in three, and monophasic in five. For the assessment of neuropathy, the Global Neurological Disability Score (GNDS) was used to initially assess the motor neurological disability, sensory loss and areflexia on a scale of 1 to 15 [9]. The GNDS scores before treatment were 12.5±3.0 (mean±SD, range: 6–15). On nerve conduction studies, motor nerve conduction velocities (MCV) were all reduced in all patients in at least more than one nerve. Sensory nerve conduction velocities (SCV) were normal in 5/18, unevoked in 7/18 and reduced in 6/18 in the median nerve and normal in 4/18, unevoked in 8/18 and reduced in 4/18 in the sural nerve. Protein levels in the cerebrospinal fluid (CSF) were elevated in 13 of 17 examined (>40 mg/dl) while none had CSF pleocytosis. All but one patient were subjected to immunotherapies and a 2-point decrease in the GNDS score was considered to be effective. Seven of 17 patients (41.1%) responded to immunotherapies; high-dose corticosteroids (prednisolone 40–60 mg/day with gradual taper) were effective in two of four patients who received it, IVIg was effective in three of five patients, and plasma exchange (PE) was effective in two of five. Three patients who received PE and IVIg showed no

Table 1
Demographic features of patients with CIDP

Patient No.	Sex	Age at onset (year)	Age at exam. (year)	Duration (months or years)	GNDS at peak	CSF cell/ protein (/μl, mg/dl)	Clinical course	Response to immunotherapies	Clinical symptoms		Evoked potentials			
									Predominant symptoms	Symmetrical involvement	MEP abnormality		SEP abnormality	
											CNS	PNS	CNS	PNS
1	M	58	65	8y	15	3/217	R	IVIg: +	motor>sensory	+	−	+	ND	
2	M	28	28	1y	11	5/100	CP	IVIg: +	motor>>sensory	+	+	+	−	+
3	F	58	59	4m	15	0/33	CP	IVIg: +	motor>sensory	+	−	+	−	−
4	M	17	17	1y	15	1/58	CP	PE: −	motor	+	−	+	ND	
5	M	47	52	5y	15	1/34	CP	IVIg, PE: −	motor>sensory	+	−	+	ND	
6	F	51	52	1y	11	3/178	CP	PE: −	motor>sensory	+	−	+	−	−
7	M	31	32	11m	9	0/320	CP	IVIg, PE: −	motor>sensory	+	−	+	−	−
8	F	48	52	5y	15	1/55	CP	PE: +	motor>sensory	−	−	+	−	−
9	M	12	18	6y	15	0/266	CP	PE: −	motor>sensory	+	−	−	ND	
10	M	11	45	34y	9	0/67	R	CS: +	motor	+	−	+	+	−
11	M	66	67	1y	15	3/290	CP	CS: −	motor>sensory	+	ND		−	−
12	M	36	42	6y	6	3/62	R	IVIg, PE: −	motor>sensory	+	+	+	−	+
13	M	69	69	2m	13	1/57	M	PE: +	motor>sensory	+	+	+	ND	
14	F	26	26	2m	11	1/157	M	CS: +	motor	+	ND		−	+
15	M	46	46	2m	15	2/127	M	CS: −	motor>sensory	+	ND		−	−
16	M	1	37	36y	8	2/27	CP	IVIg: −	motor>sensory	+	+	+	−	+
17	M	46	46	2m	13	ND	CP	ND	motor=sensory	+	ND		−	+
18	F	72	72	2m	15	1/28	CP	IVIg: −	motor>sensory	−	ND		−	−

M: male; F: female; m: months; y: years; CSF: cerebrospinal fluid; R: relapsing–remitting; M: monophasic; CP: chronic progressive; ND: not done; GNDS: Global Neurological Disability Score.
Response to immunotherapies given.
IVIg: intravenous immunoglobulin (IVIg), PE: plasma exchange (PE), CS: corticosteroids.
+: effective (2 or >2-point decrease in GNDS scores), −: no change (<2-point decrease in GNDS scores).

Please cite this article as: Pineda AAM et al. A distinct subgroup of chronic inflammatory demyelinating polyneuropathy with CNS demyelination and a favorable response to immunotherapy. J Neurol Sci (2007), doi:10.1016/j.jns.2007.01.004

significant improvement. One patient did not undergo any treatment.

2.2. Somatosensory evoked potential recording

The SEPs were obtained by stimulating the median nerve at the wrist and the posterior tibial nerve at the ankle with frequencies of 5 Hz and 2 Hz respectively [10]. Recording electrodes were placed over Erb's point, seventh cervical vertebra, and C3′ or C4′ over the somatosensory cortex; for the lower extremities, the electrodes were placed over the 12th thoracic vertebra and Cz′. Fz was used as the reference of all electrodes. The amplifier used was a Neuropack 8 (Nihon kohden) with a bandpass of 5–2000 Hz and averaged at 500 for the uppers and 350 for the lowers. At least two trials were superimposed to establish reproducibility. The peak latencies of the responses were measured: N9 (Erb), N13 (C7) and N20 (sensory cortex) for median nerve SEPs and N20 (Th12) and P37 (sensory cortex) for tibial nerve SEPs. Central sensory conduction time (CSCT) was calculated as N20–N13 for the upper extremities while P37–N20 for the lower extremities. The normal values for SEPs in our laboratory are as follows: for the upper extremities, for median nerve stimulation, the mean for N13–N20 is 5.89 with an upper limit of 7.33 ms, while for the lower extremities, with posterior tibial nerve stimulation, the mean for N20–P37 is 16.88 ms with an upper limit of 21.83 ms, while for peroneal nerve stimulation, the mean for N13–P28 is 14.5 ms with an upper limit of 20.08 ms [10]. Latencies exceeding the mean+3SD from the established normal values for SEPs were considered abnormal.

2.3. Motor evoked potential recordings

Magnetic stimuli were applied to the motor cortex and the seventh cervical vertebra using an eight-shaped coil for the upper extremities while a double cone coil was used for stimulating the motor cortex for the lower extremities, and the lumbar root (L4) was elicited by the eight-shaped coil [11]. The target muscles were the abductor pollicis brevis for the hands and the abductor hallucis for the legs. The stimulator used was an SMN-1200 (Nihon kohden) with a stimulus intensity of 65% of stimulator output for the upper extremity and lumbar, and 90% was used for the vertex. The amplifier was a Neuropack 8 (Nihon kohden) and the bandpass of 50–3000 Hz. We assessed MEP latencies and amplitudes (qualitatively) and calculated the central motor conduction time (CMCT): CMCT=CML−PML (CML: cortical motor latency; PML: peripheral motor latency). Normal values: the normal mean central conduction used in our laboratory for the thenar muscle central conduction is 8.61 ms with an upper limit of 10.67 ms while for the plantar muscle the mean central conduction time is 16.94 ms with an upper limit of 21.04 ms [10]. Latencies exceeding the mean+3SD from the established normal values for MEPs were considered abnormal.

2.4. Magnetic resonance imaging

MRI was performed using 1.5 T units, Magnetom Vision and Symphony (Siemens Medical Systems, Erlangen, Germany) as described previously [12]. The typical imaging parameters for brain MRI were: axial T2-weighted turbo spin-echo imaging using TR/TE=2800/90 ms, flip angle=180°; axial turbo-FLAIR imaging using TI/TR/TE=2200/9000/110 ms, flip angle=180°; and sagittal and axial precontrast and axial and coronal postcontrast T1-weighted spin-echo imaging using TR/TE range=400–460/12–17 ms, flip angle range=80–90°. One excitation, with a matrix of 256×256, a slice thickness of 5 mm, and a slice gap of 2.5 mm was used for all brain studies. Gadopentetate dimeglumine at 0.1 mmol/kg body weight was administered intravenously for contrast-enhanced studies. The typical imaging parameters for the spinal cord were as follows: sagittal T2-weighted turbo spin-echo imaging using TR/TE range=2500–2800/90–116 ms, flip angle=180°, number of excitations=3–4; sagittal T1-weighted spin-echo imaging using TR/TE range=400–440/11–12 ms, flip angle range=90–170°, number of excitations=2–3; axial T2-weighted turbo spin-echo imaging using TR/TE range=3200–5360/99–116 ms, flip angle=180°, number of excitations=3–4; axial T1-weighted spin-echo imaging using TR/TE range=400–440/12 ms, flip angle range=90–170°, number of excitations=2. For sagittal imaging, a matrix of 256×256 or 512×512, a slice thickness of 4 mm and a slice gap of 0.4 mm were used, and for axial imaging, a matrix of 256×256 or 512×512, a slice thickness of 5 mm, and a slice gap range of 1.5–5 mm were used. Both brain and spinal cord MRI's were taken at the time of illness and were independently evaluated by two of the authors, one of whom (T. Yoshiura) is a neuroradiologist who was unaware of the diagnoses.

2.5. Statistical analysis

Statistical analyses were performed using the Mann–Whitney *U* test to determine significant differences in age at onset, duration of disease and CSF protein levels between the two groups and the differences in GNDS scores between those with CNS involvement and those without and between before and after treatment. Fisher's exact probability test was used for sex ratio and clinical course. The p values of <0.05 were considered to be significant.

3. Results

3.1. Electrophysiological findings

Five of the 13 patients who underwent SEPs had peripheral nerve involvement, one (Patient No. 10 in Table 1) having prolonged CSCT (8%). This patient had bilateral lower extremity involvement (peroneals) with CSCTs of 22.72 ms on the right and 23.52 ms on the left. Another patient (Patient No. 15) had unevoked N13 but prolonged N20 on median

Please cite this article as: Pineda AAM et al. A distinct subgroup of chronic inflammatory demyelinating polyneuropathy with CNS demyelination and a favorable response to immunotherapy. J Neurol Sci (2007), doi:10.1016/j.jns.2007.01.004

nerve SEPs bilaterally and was not regarded as having definite CNS involvement, though the possibility of CNS involvement was not fully ruled out. Of the 52 limbs examined, 12 (23%) showed prolonged latencies (compared with the normal values previously mentioned) for Erb (N9), and the seventh cervical vertebrae (N13) for the upper extremities and fourth lumbar vertebrae (N17) and twelfth thoracic vertebrae (N20) for the lower extremities with posterior tibial nerve stimulation. Of the 13 patients who underwent MEP, 12 showed peripheral involvement and four had abnormal CMCT (31%) (Table 1). Three of these four patients had unilateral involvement (left upper extremity with a CMCT of 10.8 ms, right lower extremity with a CMCT of 23.5 ms and left lower extremity with a CMCT of 39.6 ms) while one patient had bilateral lower extremity involvement with CMCT of 26.6 ms on the right and 28.4 ms on the left. Five additional patients showed unevoked MEPs at cervical or lumbar stimulation but prolonged latency of MEPs at cortical stimulation, and were not considered to have definite CNS involvement, though the possibility of CNS involvement was not completely excluded. Of the 52 limbs examined, 31 (60%) showed prolonged latencies with Erb, cervical or lumbar stimulation as compared with normal values.

3.2. Magnetic resonance imaging findings

On brain MRI, five of 18 patients had an abnormal MRI scan; of these, four were aged 50 years or older. One patient (Patient No. 13 in Table 1, 69 years old) with abnormal CMCT, showed punctate T2 prolonged lesions in the cerebral white matter on MRI, which were considered to be non-specific. In the other three patients without CMCT or CSCT abnormalities, one (Patient No. 3, 59 years old) showed T2 prolonged lesions in the right putamen and caudate nucleus suggestive of old small infarcts while the other two (Patients No. 6, 52 years old and No. 8, 52 years old) had tiny spots of T2 prolonged lesions in the white matter on cranial MRI, which were also considered non-specific. Patient No. 17, a 46-year-old male, on fluid-attenuated inversion recovery (FLAIR) imaging, showed multiple ovoid lesions of increased signal intensity in the corpus callosum bilaterally, and in the left parietal and occipital lobes which appeared MS-like (Fig. 1).

3.3. Clinical characteristics of patients with subclinical CNS involvement

For comparison of clinical features, we divided the patients by electrophysiologic and MRI findings into two groups, those with and those without subclinical CNS involvement; patients were regarded as having subclinical

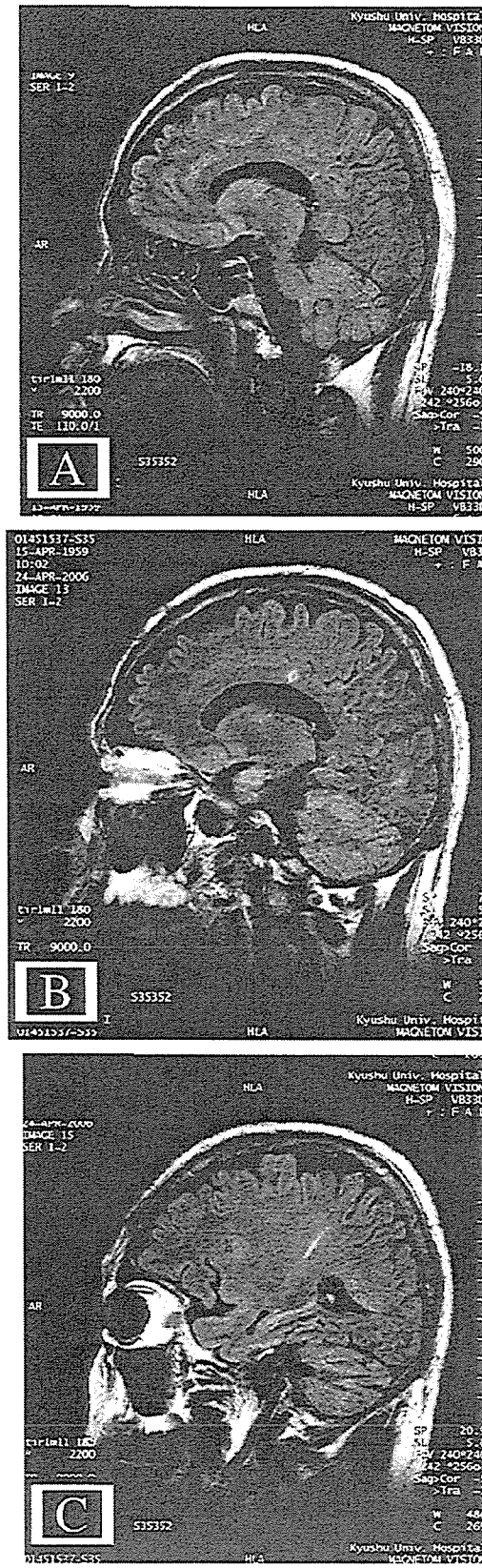

Fig. 1. Brain MRI of Patient No. 17. Sagittal fluid-attenuated inversion recovery (FLAIR) images (TR=9000 ms, TE=110 ms) of a 46-year-old male demonstrating multiple ovoid lesions of increased signal intensity in the corpus callosum, bilaterally, and in the left parietal and occipital lobes which appeared MS-like. [A] to [C]: right to left side of the patient.

Please cite this article as: Pineda AAM et al. A distinct subgroup of chronic inflammatory demyelinating polyneuropathy with CNS demyelination and a favorable response to immunotherapy. J Neurol Sci (2007), doi:10.1016/j.jns.2007.01.004

demyelinative CNS involvement if they had prolonged CMCT or CSCT or MRI lesions suggestive of CNS demyelination (MS-like ovoid lesions). Based on the electrophysiological and MRI findings, six were considered to have subclinical demyelinative CNS involvement (Patient Nos. 2, 10, 12, 13, 16 and 17) and the other 11 were not. As shown in Table 2, the patients with subclinical CNS involvement showed a tendency of male preponderance ($p=0.0537$) and significantly lower GNDS scores before treatment ($p=0.0061$), as compared with those without CNS involvement. Most patients (83%) without CNS involvement showed a chronic progressive course while half of those with subclinical CNS involvement had either a relapsing–remitting or a monophasic course. In addition, the patients with subclinical CNS involvement had lower CSF protein levels than those without, but this was not statistically significant. In the peripheral nerve conduction study, CMAP amplitude in the median nerve was significantly larger in the patients with subclinical CNS involvement than those without ($p=0.005$). In addition, in half of CIDP patients without CNS involvement, tibial nerve CMAPs were unevoked while only one of six CIDP with subclinical CNS involvement were. Patients with subclinical CNS involvement showed a nearly significant decrease of GNDS scores after immunotherapy ($p=0.0556$) while the decrease of GNDS scores was not significant in those without CNS involvement (Table 2). GNDS scores after treatment were also significantly lower in the patients with subclinical CNS involvement than in those without ($p=0.0365$).

Table 2
Comparison of clinical findings between patients with subclinical CNS involvement by EP or MRI and those without

	CIDP with subclinical CNS involvement by EP or MRI ($n=6$)	CIDP without CNS involvement ($n=12$)
Male:female	6:0	6:6
Age at onset (mean±SD, years)	31.8±24.5	44.4±19.1
Duration of disease (range, median)	2m–34y 3.5y	2m–36y 1y
Clinical course/onset		
Chronic progressive	3 (50%)	10 (83%)
Relapsing–remitting	2	1
Monophasic	1	1
GNDS before treatment	9.4±2.7*	13.8±2.2
GNDS after treatment	5.8±1.8*	11.1±4.6
CSF protein	62.6±26.1	146.9±107.5
Median nerve		
MCV, m/s	34.7±13.5	29.8±14.2
DL, ms	6.6±3.0	7.6±3.8
CMAP, mV	15.4±7.0*	5.8±3.2
Unevoked	0/6	0/12
Tibial nerve		
MCV, m/s	35.7±5.2	29.5±10.4
DL, ms	5.6±2.5	11.6±6.9
CMAP, mV	5.9±4.7	4.3±6.2
Unevoked	1/6	6/12

GNDS: Global Neurological Disability Score; CSF: cerebrospinal fluid; MCV: motor nerve conduction velocity; DL: distal latency; CMAP: compound muscle action potential. One patient from the CNS involvement group declined to have a lumbar puncture and also did not receive any immunotherapeutic intervention.
* $p<0.05$.

4. Discussion

The present study revealed subclinical CNS involvement suggestive of demyelination in Japanese patients with CIDP by combined electrophysiological and neuroimaging studies. We further described the distinct clinical features between those with and those without subclinical CNS involvement; CIDP patients with subclinical CNS involvement had lower disability and a more favorable response to immunological treatment than those without.

Although the frequent occurrence of peripheral conduction abnormalities in CIDP patients may well decrease the detection rate of CNS abnormality by EP, in the present study, about 30% of the CIDP patients demonstrated prolongation in either CMCT or CSCT, suggesting the presence of simultaneous CNS demyelination. The frequency of CNS abnormalities on EP in the present study is compatible with that reported in the previous studies [3,13]. However, though Mendell et al. [4] reported that approximately 40% of CIDP patients had MS-like periventricular, subcortical and brainstem lesions on MRI in their selected patient series, MS-like periventricular ovoid lesions were seen in only one patient in our series. Our findings are in accord with the report of Feasby et al. [5] that typical MS-like lesions are uncommon in CIDP. Our results are also compatible with those of Pąkalnis et al. [13], who concluded that with a combined EP and MRI study, EP is more sensitive than MRI in detecting CNS demyelination in CIDP. Therefore, we consider that subclinical CNS involvement is not infrequent on EPs while typical MS-like lesions suggestive of demyelination on MRI are exceptional in Japanese patients. It is suggested that a combined peripheral and central nervous system demyelination is not rare, but the nature and mechanism of CNS demyelination in CIDP is probably distinct from those in MS.

Neither characteristic clinical features nor response to immunotherapies has yet to be described in CIDP patients with subclinical CNS involvement. In our series, although the number of patients is limited, it was shown that those with subclinical CNS involvement had a milder disease, and chronic progressive disease was less frequent compared with those without CNS involvement, and showed a favorable response to immunotherapies. Although therapeutic modalities were not controlled in the present study, it has been shown that IVIg, PE and corticosteroids have essentially the same efficacy in CIDP [14,15]. In previous studies, axonal loss, as shown by a decrease in CMAP or nerve biopsy, was correlated with a significantly poor response to immunotherapies such as IVIg [1,7]. In the present study, CMAP amplitudes in median nerve were significantly larger in CIDP patients with subclinical CNS involvement than those

Please cite this article as: Pineda AAM et al. A distinct subgroup of chronic inflammatory demyelinating polyneuropathy with CNS demyelination and a favorable response to immunotherapy. J Neurol Sci (2007), doi:10.1016/j.jns.2007.01.004

without, while in the tibial nerve, unevoked response was more frequent in the latter than in the former. These findings, although seen in a small number of patients and a generalized conclusion should be drawn with caution, are still suggestive that CIDP patients without CNS involvement suffer more severe axonal pathology than those with subclinical CNS involvement. The high frequency of chronic progressive course in those without CNS involvement may also contribute to more severe axonal damage [7]. Such difference in pathology may in part explain the difference in treatment response between the two subgroups; CIDP with subclinical CNS involvement is more demyelinative and thus responsive to immunotherapies while CIDP without CNS involvement is more axonal and less responsive to such therapies. Fee and Fleming [16] reported that IVIg resolved CNS demyelinative lesions in a case of CIDP. Thus, subclinical CNS lesions are also likely to be caused by the same immune mechanism as that involved in PNS demyelination in this condition.

The presence of a combined central and peripheral inflammatory demyelinating neuropathy has long been proposed in the literature [3,4,6]. The results of our study support such a notion. Whether CIDP with subclinical CNS demyelination is distinct from CIDP without CNS involvement in etiology and mechanism remains to be elucidated, the combined use of MEP/SEP and brain MRI may help identify a subgroup of CIDP patients with combined central and peripheral demyelination. Future immunological and pathological studies in a larger group of patients and controlled therapeutic trials on this specific subgroup of CIDP patients are called for to further clarify the mechanisms behind this debilitating disease of the human nervous system.

References

[1] Bouchard C, Lacroix C, Plante V, Adams D, Chedru F, Guglielmi JM, et al. Clinicopathologic findings and prognosis of chronic inflammatory demyelinating polyneuropathy. Neurology 1999;52:498–503.

[2] Rotta FT, Sussman AT, Bradley WG, Ram Ayyar D, Sharma KR, Shebert RT. The spectrum of chronic inflammatory demyelinating polyneuropathy. J Neurol Sci 2000;173:129–39.

[3] Ormerod IEC, Waddy HM, Kermode AG, Murray NMF, Thomas PK. Involvement of the central nervous system in chronic inflammatory demyelinating polyneuropathy: a clinical, electrophysiological and magnetic resonance imaging study. J Neurol Neurosurg Psychiatry 1990;53:789–93.

[4] Mendell JR, Kolkin S, Kissel JT, Weiss KL, Chakeres DW, Rammohan KW. Evidence from central nervous system demyelination in chronic inflammatory demyelinating polyradiculoneuropathy. Neurology 1987;37 445–1291–4.

[5] Feasby TE, Hahn AF, Koopman WJ, Lee DH. Central lesions in chronic inflammatory demyelinating polyneuropathy: an MRI study. Neurology 1990;40:476–8.

[6] Hawke SHB, Hallinan JM, Mcleod JG. Cranial magnetic resonance imaging in chronic inflammatory demyelinating polyneuropathy. J Neurol Neurosurg Psychiatry 1990;53:794–6.

[7] Iijima M, Yamamoto M, Hirayama M, Tanaka F, Kastuno M, Mori K, et al. Clinical and electrophysiologic correlates of IVIg responsiveness in CIDP. Neurology 2005;64:1471–5.

[8] Report from an Ad Hoc Subcommittee of the American Academy of Neurology AIDS Task Force. Research criteria for diagnosis of chronic inflammatory demyelinating polyneuropathy (CIDP). Neurology 1991;41:617–8.

[9] Birouk N, Gouider R, Le Guern E, Gugenheim M, Tardieu S, Maisonobe T, et al. Charcot–Marie–Tooth disease type 1A with 17p11.2 duplication; clinical and electrophysiological phenotype study and factors influencing disease severity in 119 cases. Brain 1997;120: 813–23.

[10] Suga R, Tobimatsu S, Kira J, Kato M. Motor and somatosensory evoked potential findings in HLTV-1 associated myelopathy. J Neurol Sci 1999;167:102–6.

[11] Tobimatsu S, Sun S-J, Fukui R, Kato M. Effects of sex, height and age on motor evoked potentials with magnetic stimulation. J Neurol Sci 1998;245:256–61.

[12] Su J, Osoegawa M, Matsuoka T, Minohara M, Tanaka M, Ishizu T, et al. Upregulation of vascular growth factors in multiple sclerosis: correlation with MRI findings. J Neurol Sci 2006;243:21–30.

[13] Pakalnis A, Drake ME, Barohn RJ, Chakeres DW, Mendell JR. Evoked potentials in chronic inflammatory demyelinating polyneuropathy. Arch Neurol 1988;45:1014–6.

[14] Dyck PJ, Litcy WJ, Kratz KM, Suarez GA, Low PA, Pineda AA, et al. A plasma exchange versus immune globulin infusion trial in chronic inflammatory demyelinating polyradiculoneuropathy. Ann Neurol 1994;36:838–45.

[15] Hughes RAC, Bensa S, Willison HJ, Van den Bergh P, Comi G, Illa I, Nobile-Orazio E, et al. Randomized controlled trial of intravenous immunoglobulin versus prednisolone in chronic inflammatory demyelinating polyradiculoneuropathy. Ann Neurol 2001;50:195–201.

[16] Fee DB, Fleming JO. Resolution of chronic inflammatory demyelinating poly-neuropathy-associated central nervous system lesions after treatment with intravenous immunoglobulin. JPNS 2003;8:155–8.

Please cite this article as: Pineda AAM et al. A distinct subgroup of chronic inflammatory demyelinating polyneuropathy with CNS demyelination and a favorable response to immunotherapy. J Neurol Sci (2007), doi:10.1016/j.jns.2007.01.004

Molecular Microbiology (2006) 59(1), 99–112

doi:10.1111/j.1365-2958.2005.04938.x
First published online 27 October 2005

Release of the type I secreted α-haemolysin via outer membrane vesicles from *Escherichia coli*

Carlos Balsalobre,[1*†] Jose Manuel Silván,[1] Stina Berglund,[1] Yoshimitsu Mizunoe,[2] Bernt Eric Uhlin[1] and Sun Nyunt Wai[1]

[1]*Department of Molecular Biology, Umeå University, S-90187 Umeå, Sweden.*

[2]*Department of Bacteriology, Faculty of Medical Sciences, Kyushu University, Fukuoka 812–8582, Japan.*

Summary

The α-haemolysin is an important virulence factor commonly expressed by extraintestinal pathogenic *Escherichia coli*. The secretion of the α-haemolysin is mediated by the type I secretion system and the toxin reaches the extracellular space without the formation of periplasmic intermediates presumably in a soluble form. Surprisingly, we found that a fraction of this type I secreted protein is located within outer membrane vesicles (OMVs) that are released by the bacteria. The α-haemolysin appeared very tightly associated with the OMVs as judged by dissociation assays and proteinase susceptibility tests. The α-haemolysin in OMVs was cytotoxically active and caused lysis of red blood cells. The OMVs containing the α-haemolysin were distinct from the OMVs not containing α-haemolysin, showing a lower density. Furthermore, they differed in protein composition and one component of the type I secretion system, the TolC protein, was found in the lower density vesicles. Studies of natural isolates of *E. coli* demonstrated that the localization of α-haemolysin in OMVs is a common feature among haemolytic strains. We propose an alternative pathway for the transport of the type I secreted α-haemolysin from the bacteria to the host cells during bacterial infections.

Introduction

The different protein secretion systems currently described for Gram-negative bacteria establish how secreted proteins are transported through the bacterial envelopes to the extracellular milieu, where the proteins presumably then will diffuse in a soluble form to contact the target molecules or tissues. However, recent studies have shown that transport of secreted proteins to the extracellular space may involve high-order complexes with lipid membranes structures, the outer membrane vesicles (OMVs) (Wai *et al.*, 2003). From the surface of Gram-negative bacteria there is a constant formation of OMVs, presumably as a consequence of normal bacterial growth and metabolism (Beveridge, 1999). Although the mechanism of OMVs biogenesis is not fully understood, it has been proposed that they may play a role in protein export, virulence by mediating bacterial adherence to host cells, transfer of DNA between different bacterial cells and evasion of the immune system (Shoberg and Thomas, 1993; Wai *et al.*, 1995; Kolling and Matthews, 1999; Saunders *et al.*, 1999; Horstman and Kuehn, 2002; Wai *et al.*, 2003). When OMVs are formed, the different periplasmic proteins are more or less efficiently included as luminal cargo (Kadurugamuwa and Beveridge, 1995; Horstman and Kuehn, 2000; Wai *et al.*, 2003).

Secretion by the type I secretion system involves the direct transfer of the proteins from the cytoplasm to the extracellular space without the formation of periplasmic intermediates through a contiguous protein transmembrane channel generated by the type I secretion apparatus (Felmlee and Welch, 1988; Thanabalu *et al.*, 1998). Therefore, the secretion of proteins by the type I secretion system *per se* does not require any direct interaction between the secreted protein and the cell membranes. The α-haemolysin from *Escherichia coli* is an exotoxin frequently associated with strains isolated from extraintestinal infections such as uropathogenic *E. coli* (UPEC) and it is one of the best characterized examples of bacterial proteins that are secreted by the type I secretion system. The α-haemolysin belongs to the family of RTX toxins that include several bacterial proteins with conserved protein features and common genetic organization. The synthesis, activation and secretion of the α-haemolysin are determined by the *hlyCABD* operon (Welch, 1991). The α-haemolysin is synthesized in an inactive form with a molecular weight of 110 kDa, which is activated in the cytoplasm to the haemolytically active form by HlyC, a fatty acid acyltransferase (Stanley *et al.*, 1998). The α-haemolysin is directly secreted from the cytoplasm to the extracellular space through a transmem-

Accepted 28 September, 2005. *For correspondence. E-mail cbalsalobre@ub.edu; Tel. (+34) 93 402 1492; Fax (+34) 93 403 4629. †Present address: Departament de Microbiologia, Facultat de Biologia, Universitat de Barcelona, Avgda Diagonal, 645. 08028 Barcelona, Spain.

brane channel consisting of HlyB, HlyD and TolC (Thanabalu *et al.*, 1998). The inner membrane proteins HlyB and HlyD are specific components of the transport apparatus of the α-haemolysin whereas TolC is a multifunctional protein located in the outer membrane of *E. coli* (Wandersman and Delepelaire, 1990; Thanabalu *et al.*, 1998; Koronakis, 2003). The secreted α-haemolysin has cytolytic and/or cytotoxic activity against a wide range of mammalian cell types (Lally *et al.*, 1999).

Interestingly, it has been described that a fraction of the secreted α-haemolysin from *E. coli* remains located on the bacterial cell surface (Oropeza-Wekerle *et al.*, 1989). In this work, we describe experiments aimed at determining the location of the α-haemolysin when it is secreted from *E. coli* cells. Remarkably, our findings demonstrate that a considerable portion of this type I secreted α-haemolysin is associated with OMVs and that it is present there in a physiologically active form. We suggest that OMVs may play an important role in the transport/dissemination of the α-haemolysin to the host cells tissue during bacterial infections.

Results

A fraction of the secreted α-haemolysin is associated with bacterial vesicles

To further localize the α-haemolysin upon secretion we decided to investigate whether the secreted α-haemolysin was associated with vesicles. The vesicles from cultures of the α-haemolysin producing strain MC1061/pANN202-312R and the strain MC1061/pACYC184 (vector control) were isolated and analysed by electrophoresis. The isolation procedure includes removing bacterial cells by filtration of the culture supernatant and an ultracentrifugation step to collect vesicles from the cell-free culture supernatant (see *Experimental procedures* for details). The results (Fig. 1A) revealed a major band of an estimated molecular weight of 110 kDa detected in the vesicles isolated from MC1061/pANN202-312R, corresponding presumably to the α-haemolysin. That band was also detected in the whole cell extract from the same strain. Furthermore, there was no such band detected neither in the vesicles nor in the whole cell extract from the control strain. By immunoblot analysis with specific polyclonal anti α-haemolysin antiserum, we confirmed that the detected band represented the α-haemolysin (Fig. 1B). Ultrastructural analysis of vesicles was performed by electron microscopy (EM). The vesicles produced by the strain MC1061/pACYC184 were homogeneous in both size (average diameter of 50 nm) and morphology (Fig. 1C). On the other hand, the vesicles produced by the strain MC1061/pANN202-312R, which expressed the α-haemolysin, were heterogeneous (Fig. 1D). Two different subpopulations of vesicles were detected: (i) smaller vesicles that resemble in size and morphology those observed in the samples of MC1061/pACYC184; and (ii) larger vesicles (average diameter of 150 nm) with a thinner margin, indicated with arrows in Fig. 1D. Taken together, these results suggest that the secreted α-haemolysin is present not only as a soluble secreted form, but also associated with vesicles. In order to study the relevance of this finding in relation to the current model of secretion and transport of the α-haemolysin we considered that it would be of interest to estimate what percentage of the secreted α-haemolysin was vesicle-associated. To test this, the amount of (i) total secreted α-haemolysin in cell-free supernatants (before isolation of vesicles); (ii) soluble α-haemolysin (cell-free supernatant after removal of the vesicles by centrifugation); and (iii) vesicle-associated α-haemolysin (vesicles collected by centrifugation) were determined for three independent cultures of the strain MC1061/pANN202-312R. For each culture the amount of total secreted α-haemolysin was given arbitrarily the value of 100. The results, given as a percentage, indicated that most of the secreted α-haemolysin was

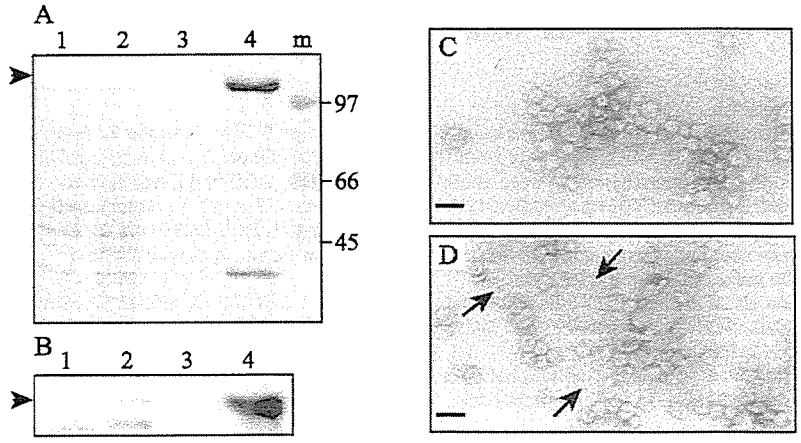

Fig. 1. The α-haemolysin is present in vesicles.
A. Electrophoretical analysis of whole cell extract (lanes 1, 2) and vesicles (lanes 3, 4) of MC1061/pACYC184 (lanes 1, 3) and MC1061/pANN202-312R (lanes 2, 4) cultures. Coomassie blue stained 10% SDS-PAGE. Lane m: molecular mass markers (size in kDa indicated along the right side). The band corresponding to the α-haemolysin is indicated with an arrowhead.
B. Immunoblot analysis of the same samples as in A using anti-α-haemolysin antibodies.
C and D. Electron micrographs of MC1061/pACYC184 (C) and MC1061/pANN202-312R (D) vesicles, bar equal to 100 nm.

associated with vesicles (66 ± 6%), whereas a smaller fraction was present in a free soluble form in the supernatant (34 ± 6%).

The α-haemolysin is tightly associated to vesicles

The above results could indicate that either the α-haemolysin was physically associated with the vesicles or alternatively that the α-haemolysin copurified together with the vesicles. To distinguish between the two possibilities dissociation assays were performed (Fig. 2A). Treatment of the vesicles with high salt concentration (either 1 M NaCl or 0.1 M Na_2CO_3) did not extract the α-haemolysin from the vesicles to any greater extent than that observed with HEPES buffer alone. Treatment with urea (0.8 M) did not affect the vesicle association of the α-haemolysin (Fig. 2A). Moreover, dissociation assays with increasing concentrations of urea (1.5 and 8 M) showed that the interaction of the α-haemolysin with the vesicles was highly resistant to the urea treatment (Fig. S1, *Supplementary material*). We conclude that protein aggregation could not be the reason for the presence of the α-haemolysin in the vesicle preparation. However, treatment with non-ionic detergent (0.5% Triton X-100) liberated all the α-haemolysin to the supernatant as a result of the vesicle membrane disruption. Control experiments using soluble α-haemolysin did rule out the possibility that the α-haemolysin simply precipitated in presence of the high

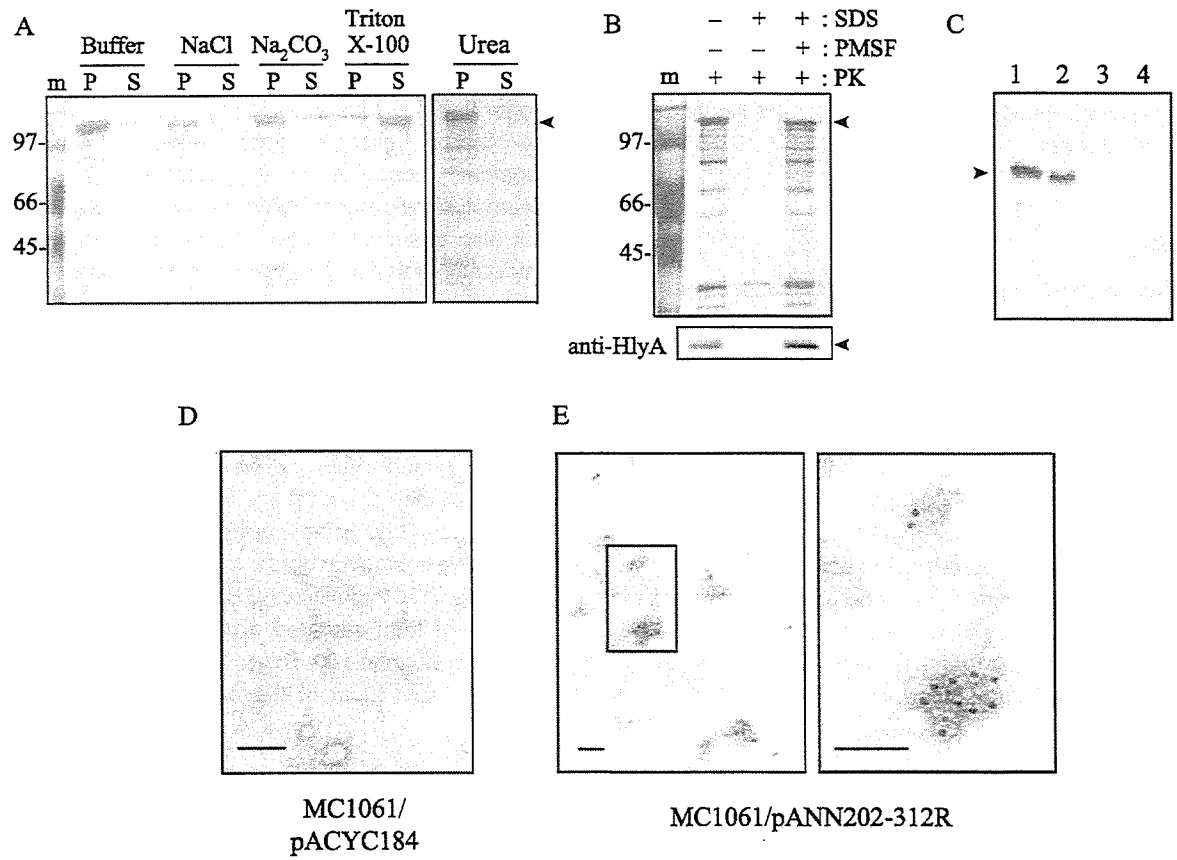

Fig. 2. The α-haemolysin is tightly associated with the vesicles.
A. Dissociation assays using vesicles from MC1061/pANN202-312R. Samples of vesicles in 20 mM Tris HCl pH 8.0 were treated for 60 min on ice in presence of: 20 mM Tris HCl pH 8.0 (buffer) or NaCl (1 M) or Na_2CO_3 (0.1 M) or Urea (0.8 M) or TritonX-100 (0.5%) respectively. The samples were then centrifuged and the resulting pellets (P) and supernatants (S) were analysed by 10% SDS-PAGE and Silver stained.
B. Proteinase K susceptibility assay. Equal amounts of vesicles from MC1061/pANN202-312R were treated with 0.5 μg ml^{-1} of proteinase K (PK). When indicated 1% SDS and 1 mM PMSF, a proteinase K inhibitor, were added. Samples were analysed in 10% SDS-PAGE and either silver stained (upper panel) or subjected to immunoblot analysis using polyclonal anti-α-haemolysin serum (bottom panel). In A and B lane m corresponds to the molecular mass markers (size in kDa indicated along the left side).
C. Immunoblot analysis using the monoclonal anti-α-haemolysin antibody E2 of the whole cell extract (lanes 1 and 3) and vesicles preparations (lanes 2 and 4) of cultures of the strains MC1061/pANN202-312R (lanes 1 and 2) and MC1061/pACYC184 (lanes 2 and 4). In A–C the band corresponding to the α-haemolysin is indicated with an arrowhead.
D–E. Immunogold-labelling (10 nm diameter gold particles) of HlyA using the monoclonal antibody E2 and vesicle preparations isolated from the strains MC1061/pACYC184 (Fig. 2D) and MC1061/pANN202-312R (Fig. 2E). The right panel in Fig. 2E is an enlargement of the indicated area in the left panel. Bars: 100 nm.

concentration of salts and thereby was recovered together with the vesicles (data not shown). Therefore, we conclude that the α-haemolysin was associated tightly with the vesicles and only when the membrane structure was disrupted did the toxin appear in soluble form. Proteinase K protection assays supported the above results. As shown in Fig. 2B, when vesicles from MC1061/pANN202-312R were incubated with Proteinase K in presence or absence of SDS, proteolytic digestion of the α-haemolysin was detected in presence of detergent (1% SDS) but no, or very little, digestion occurred in absence of the membrane disrupting agents, indicating that the α-haemolysin was partially protected by the vesicle structure. Control experiments using soluble α-haemolysin showed that the protein was proteinase K-sensitive both in presence or absence of the detergent.

In order to test if free α-haemolysin might readily attach to OMVs, experiments were performed where purified α-haemolysin was mixed with OMVs from a non-haemolytic strain (MC1061/pACYC184). However, no spontaneous association of the soluble α-haemolysin with the OMVs from MC1061/pACYC184 was detected (data not shown).

Electron microscopy analyses by immunogold-labelling of HlyA in vesicle preparations from the strains MC1061/pACYC184 and MC1061/pANN202-312R were performed using an anti-HlyA monoclonal antibody. As shown by Western blot, the antibody specifically recognized the α-haemolysin in both total cell extract and vesicle preparations from the strain MC1061/pANN202-312R and did not cross-react with proteins from the control strain MC1061/pACYC184 (Fig. 2C). Furthermore, in the EM analyses a positive gold labelling was only detected in case of the vesicle preparations from strain MC1061/pANN202-312R (Fig. 2D and E). Interestingly, no gold deposition was found in areas with intact vesicles but intense deposition of gold particles was detected only in areas where vesicles structures seemed disrupted. (Fig. 2E).

The vesicles produced by haemolytic strains are OMVs

Presumably different kinds of vesicles could in principle be produced by Gram-negative bacteria: vesicles containing both outer and inner membranes and vesicles containing only either type of membrane. To determine the nature of the vesicles from the strain MC1061/pANN202-312R we monitored the presence of specific protein markers for the outer membrane, inner membrane and the cytosol (Fig. 3). The presence of two outer membrane proteins, OmpA and TolC, was detected using specific polyclonal antibodies in both whole cell extract and vesicles from MC1061/pANN202-312R. To detect the presence of inner membrane in vesicle preparations, the NADH oxidase activity, a well established inner membrane marker was determined. As controls, both outer and inner membranes

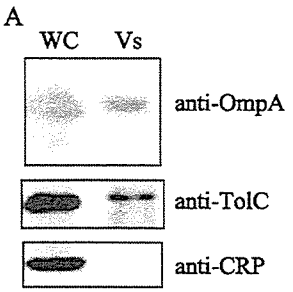

B

NADH oxydase activity (mM/min x μg protein)	
IM	1.21
OM	0.21
Vs	0.018

Fig. 3. Composition of the vesicles produced by MC1061/pANN202-312R.
A. Immunoblot analyses of both whole cells extract (WC) and vesicles preparations (Vs) from cultures of MC1061/pANN202-312R using the specific antisera indicated. WC was loaded the equivalent to 75 μl of a culture with an OD_{600} of 0.8; Vs was loaded the vesicles recovered from 4 ml of a culture with an OD_{600} of 0.8.
B. NADH oxidase- specific activity of inner membrane (IM), outer membrane (OM) and vesicle (Vs) preparations of MC1061/pANN202-312R.

were isolated from MC1061/pANN202-312R. The specific NADH oxidase activity detected in vesicle preparations was very low when compared with the inner membrane fractions. Furthermore, immunoblotting indicated that the cytoplasmic protein CRP was absent from the vesicles. These results strongly indicated the absence of inner membrane in the vesicles and we conclude that the vesicles from α-haemolysin-producing *E. coli* were OMVs.

The α-haemolysin associated with OMVs is active

To investigate if the α-haemolysin associated with OMVs was active we tested it in different assays. The cytolytic activity against red blood cells was tested by measuring the release of haemoglobin after co-incubation of horse blood with OMVs from both MC1061/pACYC184 and MC1061/pANN202-312R strains. The results (Fig. 4A) provided clear evidence for cytolytic activity associated with the OMVs from MC1061/pANN202-312R but there was little or no such activity in the OMVs from MC1061/pACYC184. Furthermore, virtually no haemoglobin release was detected in absence of calcium, which is consistent with the fact that the activity of the α-haemolysin is calcium-dependent. The activity of the α-haemolysin associated with OMVs was also tested on nucleated cells by monitoring the induction of cell detachment using HeLa cells monolayers. When testing either the bacterial cultures or the cell-free supernatants (including OMVs) from the strain MC1061/pANN202-312R we observed massive loss of the HeLa cell monolayer, more than 50% of the cells were detached after 90 min (Fig. 4B). A similar level of cell monolayer disruption was observed when OMVs from the α-haemolysin producing bacteria were tested. In contrast, no disturbance of the HeLa cell monolayer was observed when samples of the negative control

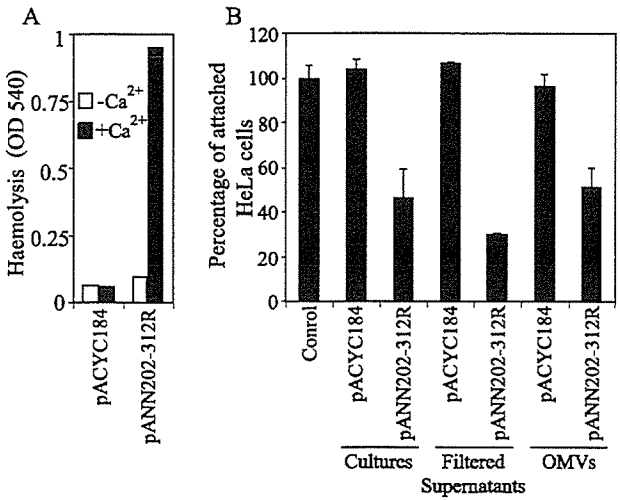

Fig. 4. The α-haemolysin present in OMVs is active.
A. Haemolytic activity of OMVs isolated from cultures of MC1061/pACYC184 and MC1061/pANN202-312R in either the absence (grey bars) or the presence (black bars) of 10 mM $CaCl_2$.
B. HeLa cell monolayer detachment activity. Percentage of remaining attached HeLa cells, measured as OD_{590}, after 90 min incubation in presence of either bacterial culture or filtered supernatant or OMVs preparation from strains MC1061/pACYC184 and MC1061/pANN202-312R. The results are the average of three independent experiments. For each experiment the OD_{590} after incubation in presence of buffer (control) was given arbitrarily the value 100. The error bars indicate the standard deviation among the experiments.

strain MC1061/pACYC184 were tested. Taken together, these results confirm that the α-haemolysin present in OMVs was active in both lytic (on red blood cells) and non-lytic (on HeLa cells) assay systems.

The localization of the α-haemolysin in OMVs is independent of the HlyC-mediated fatty acid acylation

The activity of the α-haemolysin is strictly dependent of a fatty acid acylation catalysed by HlyC in the cytoplasm. Previously, it has been described that the acylation is not required for the secretion of the α-haemolysin (Stanley *et al.*, 1998). To find out whether the localization of the α-haemolysin in OMVs requires this post-translational modification, OMVs from strains W3110/pANN202-812 (*hlyA*$^+$*hlyC*$^-$), W3110/pANN202-812B (*hlyA*$^+$*hlyC*) and W3110/pBR322 (vector control) were isolated and analysed both electrophoretically and by EM. The results (Fig. 5A) indicated that both the acylated α-haemolysin and the non-acylated α-haemolysin were present in the OMVs. EM analysis showed that OMVs containing the non-acylated α-haemolysin (from strain W3110/pANN202-812B, *hlyA*$^+$*hlyC*) appeared identical to the OMVs containing acylated α-haemolysin (Figs 5B and 1D). We here show results obtained with the *E. coli* K-12 strain W3110 background. The results with strain MC1061/pANN202-812B were completely consistent (data not shown). This comparison also thereby verified that the findings on HlyA in OMVs obtained with the MC1061 derivatives were not a strain-specific phenomenon. We conclude that the association of the α-haemolysin to OMVs is independent of the HlyC-mediated fatty acid acylation.

It was earlier shown that haemolysin is, after synthesis, rapidly detected in culture supernatants (Felmlee and Welch, 1988). To study the kinetics of the localization of newly synthesized α-haemolysin in OMVs, proteins were labelled by a 20 s pulse of radiolabelled methionine and soluble and OMVs fractions from supernatants of MC1061/pANN202-312R cultures were analysed (see *Experimental procedures* for details). Newly synthesized α-haemolysin was appearing within 20 s labelling period in both fractions: OMVs and soluble (Fig. 6). The result shown is fully consistent with the data on the kinetics of total secreted α-haemolysin previously published (Felmlee and Welch, 1988) and suggests a very quick association of the newly synthesized α-haemolysin with the OMVs. Furthermore, a quantification of the radiolabelled α-haemolysin in OMVs and in the soluble form showed that a great majority (> 90%) of the newly synthesized α-haemolysin was associated with the OMVs and thereby the result was consistent with previous estimations.

A particular feature of the secretion of the α-haemolysin is that it is dependent on a domain located in the carboxy terminal domain of the protein. It is known that the 23 kDa carboxy terminal domain of the α-haemolysin is sufficient for the export through the membranes (Nicaud *et al.*, 1986). Experiments with an epitope-tagged construct

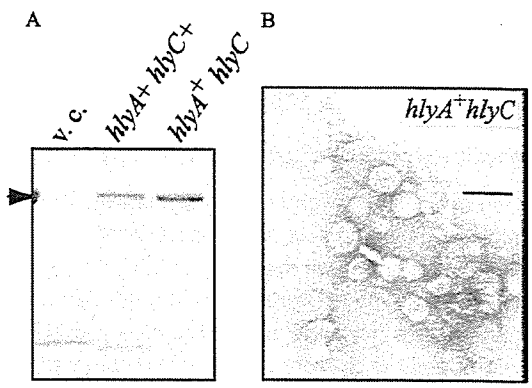

Fig. 5. The localization of the α-haemolysin in OMVs is independent of the HlyC-mediated acylation.
A. Electrophoretical analysis (Coomassie stained 10% SDS-PAGE) of the OMVs preparations of the strains W3110/pBR322 (vector control, v.c), W3110/pANN202-812 (*hlyA*$^+$ *hlyC*$^-$) and W3110/pANN202-812B (*hlyA*$^+$ *hlyC*). The band corresponding to the α-haemolysin is indicated by an arrowhead.
B. Electron micrographs of W3110/pANN202-812B OMVs. Bar: 100 nm.

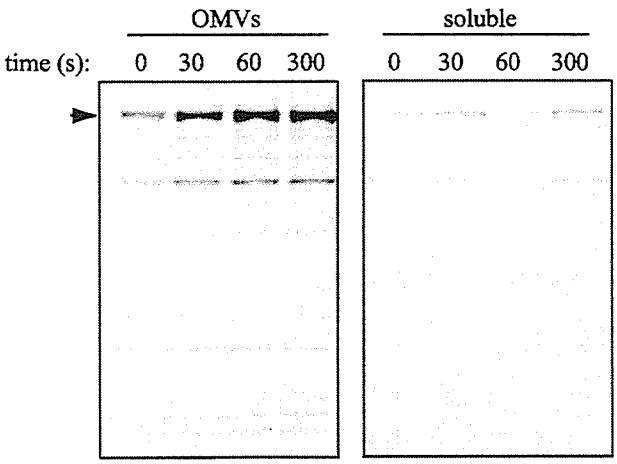

Fig. 6. The localization of the α-haemolysin in OMVs is very fast after synthesis and secretion. Electrophoretical analysis (10% SDS-PAGE) of the OMVs and soluble fractions of the supernatant of cultures of the strain MC1061/pANN202-312R after [^{35}S]Methionine was incorporated for 20 s. The length of the chase period is indicated at the top in seconds. The band that was identified by immunoblot as the α-haemolysin (data not shown) is indicated with an arrowhead.

of the 23 kDa C-terminal secretion signal of the α-haemolysin (Fernandez *et al.*, 2000) were performed to investigate whether the carboxy terminal domain itself also could determine the localization of the α-haemolysin in the OMVs. The results obtained indicated that this domain, which is essential for its secretion, is not sufficient for its localization in the OMVs (Fig. S2, *Supplementary material*).

Altered protein composition and morphology of α-haemolysin containing OMVs

The presence of a fraction of larger OMVs in the preparations of MC1061/pANN202-3012R but not in MC1061/pACYC184 (Fig. 1) led us to hypothesize that the larger OMVs harboured the α-haemolysin. To test this hypothesis, the OMVs from MC1061/pANN202-312R were fractionated in a density gradient and the fractions obtained were analysed for the protein composition (Fig. 7A). The protein bands corresponding to OmpA and the α-haemolysin were identified by Western blotting (data not shown) and the relative content of these proteins in the different fractions was quantified and plotted (Fig. 7B). The gradient profile of OmpA indicated the existence of two populations of OMVs with different density that peaked in fractions No. 9 and No. 15 respectively. The detection of lipopolysaccharide (LPS) by silver staining after SDS-PAGE analysis of the different Optiprep gradient fractions also suggested that OMVs were distributed in the density gradient as two peaks around fractions No. 9 and No. 15 respectively (data not shown). Interestingly, most of the α-haemolysin (> 70%) was present in the same fractions as the low-density OMVs (fractions 9–10). When the calcium-dependent cytolytic activity against red blood cells was monitored (Fig. 7C), the maximal activity was detected, as expected, in case of the fractions containing the α-haemolysin-enriched OMVs. Notably, the TolC protein, the outer-membrane component of the type I secretion machinery, was only detected in the fractions containing the majority of the α-haemolysin. In fact, more than 95% of the total TolC was found in the fractions No. 9 and No. 10 by immunoblot analysis (Fig. 7D). The absence of detectable TolC in the fractions No. 14 and No. 15, which contained similar amounts of OmpA protein, indicates a differential protein composition of the OMVs containing α-haemolysin versus the OMVs not containing α-haemolysin. Silver staining analyses of the protein content of the fractions No. 9 and No. 15 revealed additional differences in the protein composition (Fig. 7E). Similar protein profiles as that of fractions No. 9 and No. 15 were observed in the case of fractions No. 10 and No. 14 respectively (data not shown). Thin-layer chromatography (TLC) studies indicated that the phospholipids composition was not altered in the OMVs of strains producing α-haemolysin when compared with the control strain. Furthermore, no significant differences in the phospholipids composition were detected between the two population of OMVs separated by fractionation in a density gradient, fractions No. 9 and No. 15 (Fig. S3, *Supplementary material*).

Electron microscopy analyses were performed on fractions No. 9 and No. 15 as well as on the OMVs sample used for the vesicle fractionation (input). As shown in Fig. 7F the vesicle preparation from MC1061/pANN202-312R (input) contained two clearly different subpopulations of OMVs (see also Fig. 1D). In the fraction No. 9 we observed a clear enrichment of the larger OMVs with thinner margin that were only detected in preparations from strains producing α-haemolysin. By using the difference in size among OMVs, we could estimate that in the input the amount of large OMVs (> 150 nm) was approximately 4% ($n = 1200$), although in the fraction No. 9 it was approximately 25% ($n = 190$). Moreover, most of small OMVs (< 150 nm) observed in the fraction No. 9 had the thinner margin . like that observed in case of the large OMVs and different from the appearance of the margin of the OMVs recovered in fraction No. 15. Furthermore, most of the OMVs present in the fraction No. 15 resembled the vesicles that were detected in OMVs preparations from the control strain. As most of the α-haemolysin and the haemolytic activity were detected in fraction No. 9 we concluded that these low density vesicles are the ones containing the α-haemolysin. When OMVs from the strain MC1061/pACYC184 (vector control) were fractionated in an

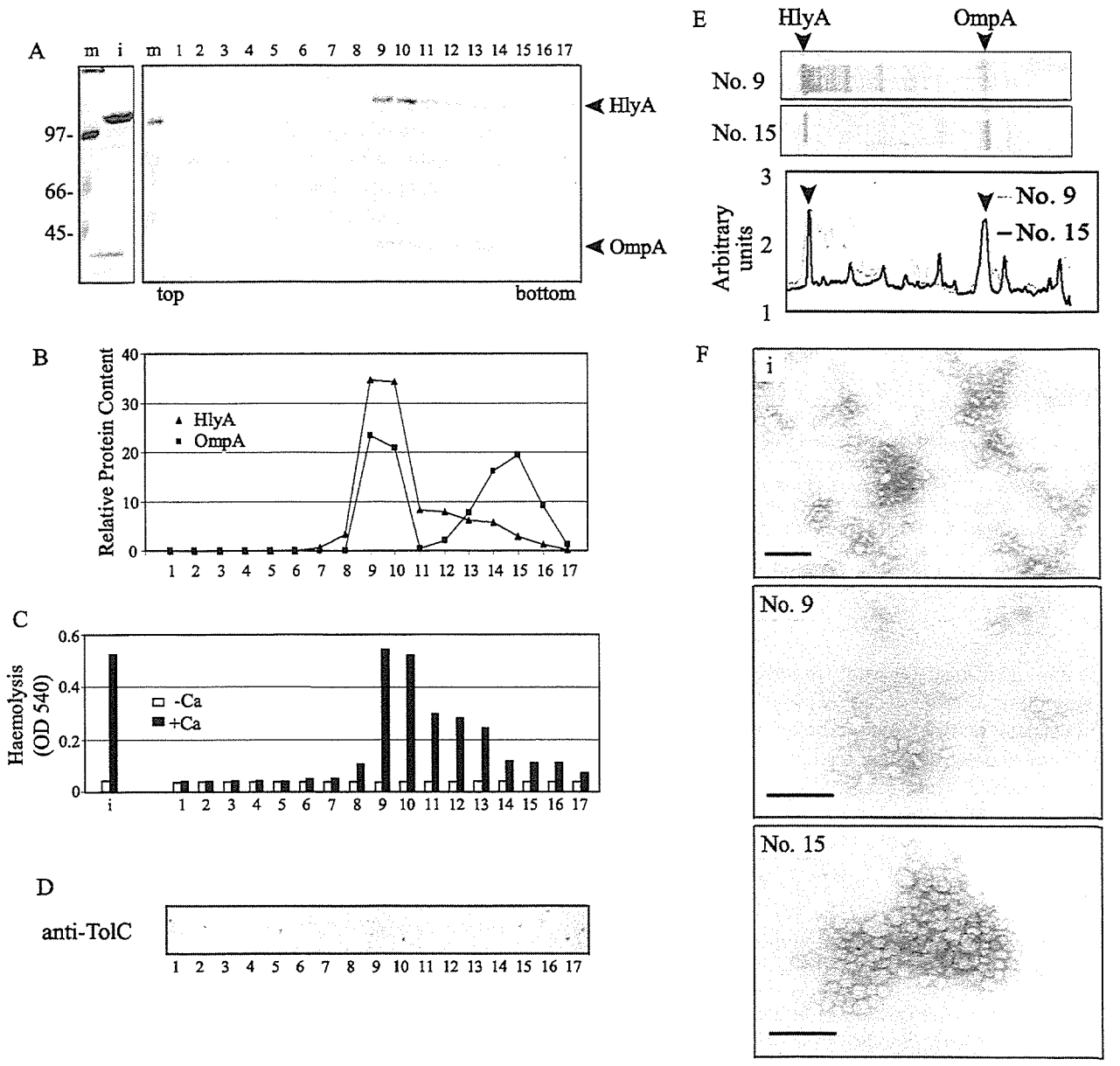

Fig. 7. Density gradient fractionation of OMVs from MC1061/pANN202-312R.
A. Electrophoretical analysis (Coomassie stained 10% SDS-PAGE) of the density gradient fractions from top (No. 1, lowest density) to bottom (No. 17, highest density) from MC1061/pANN202-312R OMVs. The bands corresponding to the α-haemolysin and OmpA are indicated. Lane m, molecular mass markers (size in kDa indicated along the left side); lane i, input OMVs from MC1061/pANN202-312R.
B. The quantification of the amounts of α-haemolysin (triangles) and OmpA (squares) in the different fractions was performed by densitometry and plotted on a relative scale.
C. Haemolytic activity of the gradients fractions from A either in presence (black bars) or in absence (grey bars) of calcium. The haemolytic activity of the input is shown by the leftmost columns (i).
D. Immunoblot analysis of the different fractions using anti-TolC serum.
E. Silver staining analysis after 10% SDS-PAGE of the proteins present in fractions No. 9 and No. 15. A densitometric analysis of the silver stained protein bands is shown in the lower panel. The bands corresponding to the α-haemolysin and OmpA are indicated by vertical arrowheads.
F. Electron micrographs of OMVs from MC1061/pANN202-312R (i: Input); fractions No. 9 and No. 15. Bar equal to 250 nm.

Optiprep gradient and OmpA was detected, a uniform population of OMVs was observed, which migrated through the gradient in a manner similar to that of the fractions No. 14–15 from the MC1061/pANN202-312-R OMVs preparations (data not shown).

Localization of secreted α-haemolysin in OMVs from different E. coli *isolates*

To determine if the transport of the α-haemolysin by OMVs was a common feature in haemolytic *E. coli* strains